

Mapping dynamical systems into chemical reactions

Tomislav Plesa ¹

Abstract: Polynomial dynamical systems (DSs) can model a wide range of physical processes. A special subset of these DSs that can model chemical reactions under mass-action kinetics is called chemical dynamical systems (CDSs). A central problem in synthetic biology is to map polynomial DSs into dynamically similar CDSs. In this paper, we introduce the *quasi-chemical map* (QCM) that can systematically solve this problem. The QCM introduces suitable state-dependent perturbations into any given polynomial DS which then becomes a CDS under sufficiently large translations of variables. This map preserves robust features, such as generic equilibria and limit cycles, as well as temporal properties, such as periods of oscillations. Furthermore, the resulting CDSs are at most one degree higher than the original DSs. We demonstrate the QCM by designing relatively simple CDSs with exotic dynamics and bifurcations, and addressing Hilbert’s 16th problem in chemistry.

1 Introduction

First-order autonomous ordinary-differential equations with polynomials on the right-hand side, which we call polynomial *dynamical systems* (DSs) [1], can model time-evolution of a range of chemical and biological processes [2, 3]. In particular, for chemical reactions under mass-action kinetics, the dependent variables in the corresponding DSs can be interpreted as (non-negative) chemical concentrations, and each distinct monomial can be interpreted as a chemical reaction [2, 3]. In this paper, this subset of DSs is called *chemical dynamical systems* (CDSs). For example, $dx/dt = (1 - x)$ is a CDS which describes how concentration $x = x(t)$ of a chemical species X changes in time t , with monomials 1 and $-x$ interpreted respectively as production $\emptyset \rightarrow X$ and degradation $X \rightarrow \emptyset$, where \emptyset denotes some neglected species. On the other hand, DS $dy/dt = -1$ is not chemical, because monomial -1 drives $y = y(t)$ to negative values, and therefore cannot be interpreted as a chemical reaction.

Problems arising in chemistry and biology are often *direct*: given a CDS, the task is to deduce some of its properties, such as number and stability of time-independent solutions (equilibria) or isolated periodic solutions (limit cycles). Conversely, in the field of synthetic biology [4], and the sub-field of DNA computing [5] in particular, the defining problem is an *inverse* one: given a property, the task is to design a CDS that displays the property [6, 7, 8, 9, 10]. This challenging problem can be approached by designing CDSs from scratch, or by suitably modifying existing DSs with desired features arising from e.g. mechanical or electronic applications. Key to both of the two approaches are special maps that can transform general DSs into CDSs, while preserving desired dynamical features [6]; in this paper, we call these transformations *chemical maps*.

Any given polynomial DS can always be mapped to a CDS via a suitable state-dependent rescaling of time [11, 12]; we call the underlying chemical map the *time-change map*. Under this map, all positive solutions of the underlying DS are preserved; however, this comes at a cost. Firstly, since time is re-scaled, temporal properties, such as periods of oscillations, are changed. Such distortions can limit usefulness of the time-change map for experimental implementations, since time-scales at which dynamical phenomena occur are often of great importance. Secondly, the right-hand side of the CDSs obtained via this map is of higher degree compared to the original

¹Department of Applied Mathematics and Theoretical Physics, University of Cambridge, Centre for Mathematical Sciences, Wilberforce Road, Cambridge, CB3 0WA, UK; e-mail: tp525@cam.ac.uk

polynomial DSs, and this increase in degree scales with the number of equations. This property of the time-change map is undesirable because the significantly higher-degree terms in the resulting CDSs are experimentally more costly to implement [13, 5].

Another map put forward for designing CDSs is the *x-factorable map* [14], which involves multiplying the right-hand side of the differential equations by their respective dependent variables. The key advantage of this map is that the resulting CDSs are of only one degree higher than the original DSs. However, despite numerous successful examples [14], to the best of author’s knowledge, there are no rigorous results in the literature that systematically characterize how the *x-factorable map* influences various dynamical features.

To bridge the gap, in this paper we introduce a novel chemical map, which we call the *quasi-chemical map* (QCM). This map systematically introduces appropriate state-dependent perturbations on the right-hand side of any given polynomial DS which then becomes a CDS under sufficiently large translations of the dependent variables. The QCM displays a number of desirable properties: firstly, the resulting CDSs are *at most* one degree higher than the original DSs. Secondly, this map preserves all dynamical features that are robust to small perturbations, such as generic equilibria and limit cycles. Finally, the QCM approximately preserves temporal properties, such as periods of oscillations. In addition, we show that, in a special case, the QCM can be seen as a correction of the *x-factorable map*, thus also clarifying validity of the latter map.

The paper is organized as follows. In Section 2, we provide some background on DSs and CDSs; more details are available in Appendix A. In Section 3, we define chemical maps, and discuss two particular examples: the time-change and *x-factorable maps*; more details are presented in Appendix B. In Section 4, we introduce the QCM and prove its properties; a generalization is presented in Appendix C. In Section 5, we apply the QCM to design CDSs with exotic dynamics and bifurcations, and to address Hilbert’s 16th problem in chemistry; further details and examples are presented in Appendices D–F. Finally, we provide a summary and discussion in Section 6; further details are presented in Appendix G.

2 Background theory

In this section, we present notation and background theory used in the paper.

Notation. The space of integers is denoted by \mathbb{Z} , while the space of real numbers by \mathbb{R} . Subscripts \geq and $>$ restrict these spaces to respectively non-negative and positive numbers; for example, \mathbb{Z}_{\geq} is the space of non-negative integers, while $\mathbb{R}_{>}$ is the space of positive real numbers. Absolute value of $x \in \mathbb{R}$ is denoted by $|x|$. Euclidean column vectors are denoted by $\mathbf{x} = (x_1, x_2, \dots, x_N)^\top \in \mathbb{R}^N$, where \cdot^\top is the transpose operator. The 1-norm of $\mathbf{x} \in \mathbb{R}^N$ is given by $\|\mathbf{x}\| = |x_1| + |x_2| + \dots + |x_N|$.

2.1 Dynamical systems

Consider ordinary-differential equations given by

$$\frac{dy_i}{dt} = f_i(y_1, y_2, \dots, y_N), \quad \text{where } f_i \in \mathbb{P}_n(\mathbb{R}^N, \mathbb{R}), \quad i = 1, 2, \dots, N, \quad (1)$$

where $\mathbb{P}_n(\mathbb{R}^N, \mathbb{R})$ is the space of all polynomial functions $f : \mathbb{R}^N \rightarrow \mathbb{R}$ of degree at most n . We interpret $t \geq 0$ as time, and note that $f_i = f_i(y_1, y_2, \dots, y_N)$ is autonomous, i.e. does not depend on time explicitly. Defining $\mathbf{y} = (y_1, y_2, \dots, y_N)^\top \in \mathbb{R}^N$ and $\mathbf{f}(\mathbf{y}) = (f_1(\mathbf{y}), f_2(\mathbf{y}), \dots, f_N(\mathbf{y}))^\top \in \mathbb{R}^N$,

system (1) can be written succinctly in a vector form as

$$\frac{d\mathbf{y}}{dt} = \mathbf{f}(\mathbf{y}), \quad \text{where } \mathbf{f} \in \mathbb{P}_n(\mathbb{R}^N, \mathbb{R}^N), \quad (2)$$

where $\mathbb{P}_n(\mathbb{R}^N, \mathbb{R}^N)$ is the space of all vector-valued functions $\mathbf{f} : \mathbb{R}^N \rightarrow \mathbb{R}^N$ whose components are polynomials of degree at most n . We call (2) a *dynamical system* (DS) with state \mathbf{y} and *vector field* \mathbf{f} . We say that DS (2) is *polynomial* with degree n and dimension N . In this paper, we focus on polynomial DSs; see Section 6 and Appendix G for a discussion on non-polynomial DSs.

Let $\mathbf{y} = \mathbf{y}(t; \mathbf{y}_0)$ be the solution of (2) satisfying the initial condition $\mathbf{y}(0) = \mathbf{y}_0 \in \mathbb{R}^N$. This solution can be represented as a trajectory in the *time-state space* $\mathbb{R}_{\geq} \times \mathbb{R}^N$, i.e. as the set $\{(t, \mathbf{y}(t; \mathbf{y}_0)) | t \geq 0\}$, or projected to the *state-space* \mathbb{R}^N , i.e. as the set $\{\mathbf{y}(t; \mathbf{y}_0) | t \geq 0\}$.

Robustness. Let us consider system

$$\frac{d\mathbf{z}}{dt} = \mathbf{f}(\mathbf{z}) + \mathbf{F}(\mathbf{z}; \mu), \quad \text{where } \mathbf{F} \in C^1(\mathbb{R}^N \times \mathbb{R}_{\geq}, \mathbb{R}^N) \text{ and } \mathbf{F}(\mathbf{z}; 0) = \mathbf{0}, \quad (3)$$

where $C^1 = C^1(\mathbb{R}^N \times \mathbb{R}_{\geq}, \mathbb{R}^N)$ is the space of all functions $\mathbf{F} : \mathbb{R}^N \times \mathbb{R}_{\geq} \rightarrow \mathbb{R}^N$ that are continuously differentiable in all arguments. For all sufficiently small $\mu > 0$, DS (3) can be interpreted as a perturbation of DS (2): a “small” perturbation \mathbf{F} has been added to the vector field \mathbf{f} . Solutions of (2) that persist under all such perturbations are of special interest.

Definition 2.1. (*Robust dynamical system*) Given a compact set $\mathbb{U} \subset \mathbb{R}^N$ in the state-space, and given any vector field $\mathbf{F} \in C^1$ with $\mathbf{F}(\mathbf{z}; 0) = \mathbf{0}$, assume that there exists $\mu_0 > 0$ such that for all $\mu \in (0, \mu_0)$ the perturbed DS (3) in \mathbb{U} is qualitatively equivalent to the unperturbed DS (2) in \mathbb{U} . Then, DS (2) is said to be robust in \mathbb{U} .

Remark. In Definition 2.1, we say that DSs (2) and (3) are qualitatively equivalent in $\mathbb{U} \subset \mathbb{R}^N$ if there exists a local change of coordinates $\mathbf{y} = \mathbf{\Phi}(\mathbf{z})$ in \mathbb{U} , where map $\mathbf{\Phi}$ is continuous, has a continuous inverse, and preserves the direction of time [1, 15]; see also Appendix A.

Remark. One can also define a *robust solution* of (2) by localizing the set \mathbb{U} from Definition 2.1. In particular, a solution of DS (2) is robust if in each of its neighborhood DS (3) with sufficiently small $\mu > 0$ has a qualitatively equivalent solution; for a more precise definition, see Appendix A.

Two important classes of solutions of DSs are hyperbolic equilibria and hyperbolic limit cycles. An equilibrium \mathbf{y}^* is a time-independent solution of (2); it is hyperbolic if other nearby solutions either exponentially move towards or away from \mathbf{y}^* . A limit cycle \mathbf{y}_τ is a time-periodic solution of (2) with period $\tau > 0$; hyperbolicity has analogous meaning as for equilibria; see Appendix A for more details. These two classes of solutions are robust [1, 15].

2.2 Chemical dynamical systems

Let us consider polynomial DS

$$\frac{d\mathbf{x}}{dt} = \mathbf{g}(\mathbf{x}), \quad \text{where } \mathbf{g} \in \mathbb{P}_n(\mathbb{R}^N, \mathbb{R}^N). \quad (4)$$

Assume that, given any non-negative initial condition, the solution of (4) is non-negative for all future times; then, DS (4) is said to be *non-negative*. In this case, the non-negative orthant is a trapping region for (4), i.e. vector field \mathbf{g} points along or inwards on the boundary of \mathbb{R}_{\geq}^N : $g_i(x_1, x_2, \dots, x_N) \geq 0$ if $x_i = 0$ and $x_k \geq 0$ for $k \neq i$. We now define a special subset of such DSs that satisfy a stronger non-negativity condition: each distinct monomial in g_i is non-negative when $x_i = 0$ and $x_k \geq 0$ for $k \neq i$. This condition ensures that each of the monomials can be interpreted as a chemical reaction, and variables x_i as chemical concentrations [2, 3].

Definition 2.2. (Chemical dynamical system) Monomial $\alpha x_1^{\nu_1} x_2^{\nu_2} \dots x_N^{\nu_N}$ of $g_i \in \mathbb{P}_n(\mathbb{R}^N, \mathbb{R})$, with $\alpha \in \mathbb{R}$ and $\nu_1, \nu_2, \dots, \nu_N \in \mathbb{Z}_{\geq}$, is chemical if $\alpha x_1^{\nu_1} x_2^{\nu_2} \dots x_N^{\nu_N} \geq 0$ for $x_i = 0$ and for all $x_k \geq 0$ with $k \neq i$. Polynomial g_i is chemical if all of its distinct monomials are chemical. Vector field $\mathbf{g} = (g_1, g_2, \dots, g_N)^\top$ is chemical if all of its component are chemical. DS (4) is called a chemical dynamical system (CDS) if its vector field is chemical. Monomials, polynomials, vector fields and dynamical systems that are not chemical are non-chemical. Spaces of all n -degree polynomial vector fields that are chemical and non-chemical are denoted respectively by $\mathbb{P}_n^C(\mathbb{R}^N, \mathbb{R}^N)$ and $\mathbb{P}_n^N(\mathbb{R}^N, \mathbb{R}^N)$.

Example. Consider the two-dimensional quadratic DS

$$\begin{aligned} \frac{dy_1}{dt} &= f_1(y_1, y_2) = -1 + 3y_1, \\ \frac{dy_2}{dt} &= f_2(y_1, y_2) = 5 + 2y_1 - y_1^2. \end{aligned} \quad (5)$$

Letting $y_1 = 0$, one gets monomial $f_1(0, y_2) = -1$, which is always negative, and hence non-chemical; therefore, f_1 is non-chemical. Similarly, letting $y_2 = 0$, one obtains polynomial $f_2(y_1, 0) = (5 + 2y_1 - y_1^2)$. Monomials 5 and $2y_1$ are non-negative when $y_1 \geq 0$, and are hence chemical; on the other hand, $-y_1^2 < 0$ when $y_1 > 0$, and is therefore non-chemical; hence, f_2 is also non-chemical. Therefore, $\mathbf{f} = (f_1, f_2)^\top \in \mathbb{P}_2^N(\mathbb{R}^2, \mathbb{R}^2)$, and DS (5) is non-chemical.

Example. Consider the two-dimensional quadratic DS

$$\begin{aligned} \frac{dy_1}{dt} &= f_1(y_1, y_2) = 1 - 2y_2 + y_2^2, \\ \frac{dy_2}{dt} &= f_2(y_1, y_2) = 1 - y_1 y_2. \end{aligned} \quad (6)$$

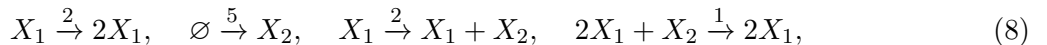
Monomials 1 and y_2^2 from $f_1(0, y_2) = (1 - 2y_2 + y_2^2)$ are chemical; however, $-2y_2$ is non-chemical, since $-2y_2 < 0$ for all $y_2 > 0$, so that f_1 is non-chemical. On the other hand, $f_2(y_1, 0) = 1 > 0$; hence, f_2 is chemical. Therefore, $\mathbf{f} \in \mathbb{P}_2^N(\mathbb{R}^2, \mathbb{R}^2)$, and DS (6) is non-chemical. However, note that DS (6) is non-negative, since $f_1(0, y_2) = (1 - y_2)^2 \geq 0$ and $f_2(y_1, 0) = 1 > 0$, i.e. \mathbb{R}_{\geq}^2 is a trapping region. This example shows that CDSs are a proper subset of non-negative DSs.

Example. Consider the two-dimensional cubic DS

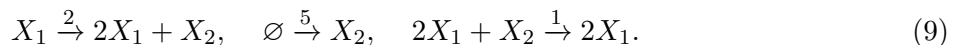
$$\begin{aligned} \frac{dx_1}{dt} &= g_1(x_1, x_2) = 2x_1, \\ \frac{dx_2}{dt} &= g_2(x_1, x_2) = 5 + 2x_1 - x_1^2 x_2. \end{aligned} \quad (7)$$

Polynomial g_1 is chemical, since $g_1(0, x_2) = 0$; similarly, g_2 is chemical, since both monomials of $g_2(x_1, 0) = (5 + 2x_1)$ are non-negative when $x_1 \geq 0$. Hence, $\mathbf{g} \in \mathbb{P}_3^C(\mathbb{R}^2, \mathbb{R}^2)$, and (7) is a CDS.

Chemical reaction networks. To every CDS one can associate a set of chemical reactions, which are jointly called a *chemical reaction network* (CRN) [3]. For example, a CRN associated with CDS (7) is given by



where X_1 and X_2 denote the chemical species whose concentrations are respectively x_1 and x_2 , and \emptyset denotes some neglected species; the positive numbers above the reaction arrows are called *rate coefficients*. Another CRN of (7) is obtained by fusing the first and third reaction in (8), and reads



See Appendix A for more details about CRNs.

3 Chemical maps

In this section, we define the central objects of this paper: maps that transform DSs (see Section 2.1) into CDSs (see Section 2.2), while preserving desired dynamical properties. Before providing a definition, let us consider a cautionary example.

Example. Consider the two-dimensional quadratic DS

$$\begin{aligned}\frac{dx_1}{dt} &= -\frac{45}{4} + \frac{1}{8}x_1 + \frac{1}{2}x_2, \\ \frac{dx_2}{dt} &= \frac{135}{8} + \frac{1}{2}x_1 - \frac{51}{32}x_2 - \frac{1}{20}x_1x_2 + \frac{1}{20}x_2^2,\end{aligned}\tag{10}$$

which has an unstable hyperbolic equilibrium $(x_1^*, x_2^*) = (10, 20)$ enclosed by a stable hyperbolic limit cycle. We displays these two features respectively as the blue dot and red curve in state-space in Figure 1(a); also shown as grey arrows is the underlying vector field. In Figure 1(b), we show the limit cycle in the (t, x_1) time-state space.

One can notice from Figure 1(a) that DS (10) is non-chemical, since the vector field can point outside the non-negative quadrant on the x_2 -axis. More precisely, (10) does not satisfy Definition 2.2 because of the non-chemical monomial $(-45/4)$ in the first equation. A naive approach to transform this DS into a CDS is to simply multiply $(-45/4)$ by x_1 , leading to

$$\begin{aligned}\frac{dx_1}{dt} &= \left(-\frac{45}{4} + \frac{1}{8}\right)x_1 + \frac{1}{2}x_2, \\ \frac{dx_2}{dt} &= \frac{135}{8} + \frac{1}{2}x_1 - \frac{51}{32}x_2 - \frac{1}{20}x_1x_2 + \frac{1}{20}x_2^2.\end{aligned}\tag{11}$$

Even though only one term of the vector field from (10) has been modified to yield (11), the underlying dynamics has been drastically changed: (11) has no equilibria and, consequently, all of its solutions grow unboundedly, i.e. we have designed a hazardous CDS. This catastrophic phenomenon, involving destruction of all non-negative equilibria and blow-up of chemical concentrations, plays an important role in molecular control [10].

Definition 3.1. (Chemical map) Consider DS (2) in a desired compact set $\mathbb{U} \subset \mathbb{R}^N$ in state-space. Consider also CDS

$$\frac{d\mathbf{x}}{dt} = \Psi\mathbf{f}(\mathbf{x}), \quad \text{where } \Psi\mathbf{f} \in \mathbb{P}_m^{\mathcal{C}}(\mathbb{R}^N, \mathbb{R}^N).\tag{12}$$

Assume that CDS (12) in some compact set $\mathbb{V} \subset \mathbb{R}_{\geq}^N$ in the non-negative orthant is qualitatively equivalent to DS (2) in \mathbb{U} . Then $\Psi : \mathbb{P}_n(\mathbb{R}^N, \mathbb{R}^N) \rightarrow \mathbb{P}_m^{\mathcal{C}}(\mathbb{R}^N, \mathbb{R}^N)$, mapping vector field \mathbf{f} to $\Psi\mathbf{f}$, is a chemical map that qualitatively preserves DS (2) in \mathbb{U} .

A natural choice for chemical maps are affine maps, since then qualitative equivalence is ensured. However, for a given DS, there is no a-priori guarantee that a suitable affine map exists. Furthermore, even if it does exist, finding this map can be a non-trivial task even for two-dimensional DSs [16], let alone higher-dimensional ones. For this reason, we do not focus on affine maps alone. In what follows, we apply two different non-affine maps to transform (10) into CDSs.

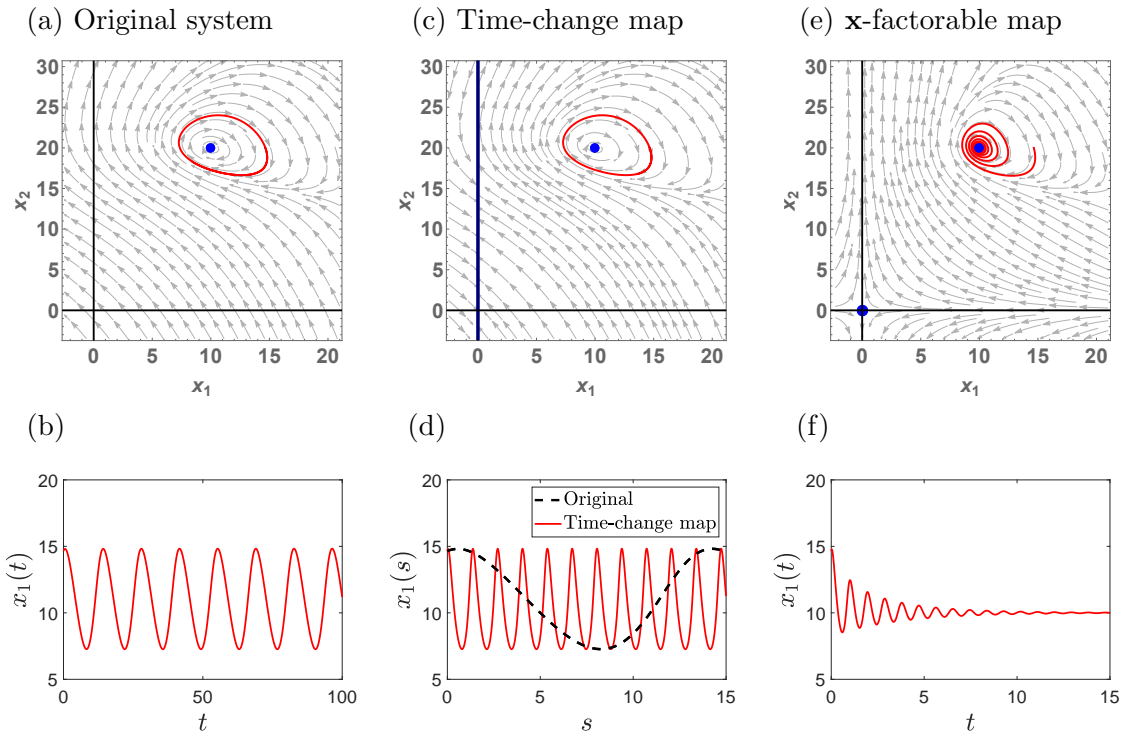


Figure 1: Application of chemical maps on DS (10). Panel (a) displays state-space for the original DS (10), with the vector field shown as gray arrows, the equilibrium as the blue dot, and the limit cycle as the red curve; panel (b) displays a corresponding (t, x_1) -space. Panels (c) and (d) show analogous plots for CDS (13), which is obtained by applying the time-change map on (10). Analogous plots are shown in panels (e) and (f) for CDS (15), which is obtained by applying the \mathbf{x} -factorable map on (10). In panel (e), shown as the blue dot at the origin is one of the boundary equilibria introduced by the \mathbf{x} -factorable map.

3.1 Time-change map

Instead of multiplying only $(-45/4)$ by x_1 , as in the naive approach (11), let us instead multiply the whole vector field from (10) by x_1 , and denote time by s , leading to the CDS

$$\begin{aligned}\frac{dx_1}{ds} &= x_1 \left(-\frac{45}{4} + \frac{1}{8}x_1 + \frac{1}{2}x_2 \right), \\ \frac{dx_2}{ds} &= x_1 \left(\frac{135}{8} + \frac{1}{2}x_1 - \frac{51}{32}x_2 - \frac{1}{20}x_1x_2 + \frac{1}{20}x_2^2 \right).\end{aligned}\quad (13)$$

We call the map that transforms DS (10) into CDS (13) a *time-change map*. More generally, the time-change map can be applied systematically as follows: assume that the first $K \geq 1$ equations from (4) are non-chemical, while the remaining $(N - K)$ equations are chemical; then, multiply *all* N components g_1, g_2, \dots, g_N of the vector field by $(x_1x_2 \dots x_K)$.

This map is equivalent to a state-dependent change of time. In particular, consider (10) with an initial condition $\mathbf{x}_0 \in \mathbb{R}_{>}^2$ such that $x_1(t; \mathbf{x}_0) > 0$ over a desired time-interval. Let us introduce a new time, given by

$$s(t) = \int_0^t \frac{d\theta}{x_1(\theta; \mathbf{x}_0)}.\quad (14)$$

Since $x_1(\theta; \mathbf{x}_0) > 0$ over the desired time-interval, $s(t)$ is then well-defined, positive and monotonically increasing; in particular, it preserves the direction of time t , and it has an inverse, which we denote by $t(s)$. Applying the chain-rule to $x_1 = x_1(t(s))$ and $x_2 = x_2(t(s))$ from (10), it follows

that $dx_1/ds = (dt/ds)dx_1/dt = x_1 dx_1/dt$ and similarly $dx_2/ds = x_1 dx_2/dt$, which yields (13). From this consideration, it follows that the time-change map is a chemical one. In particular, this map qualitatively preserves every trajectory that remains within the positive quadrant. We verify this fact in Figure 1(c), which shows state-space for (13).

However, the time change-map displays three undesirable features. Firstly, it introduces a continuum of equilibria on the x_2 -axis, which we show in blue in Figure 1(c). Consequently, for initial conditions in certain regions, the solutions of (13) asymptotically approach the x_2 -axis - a behavior qualitatively different from the original DS (10). This property arises from the fact that (14) is not differentiable at time t such that $x_1(t) = 0$. Secondly, period of oscillations is significantly changed under this map. In particular, since $x_1(t)$ oscillates around the equilibrium $x_1^* = 10$, it follows from (14) that the period is reduced roughly by a factor of 10. This observation is confirmed in Figure 1(d): we show in red the limit cycle of (13) in the (s, x_1) -space, together with the limit cycle of (10) as the black dashed curve. Finally, the time-change map in general significantly increases degree of DSs, i.e. degree m can be significantly larger than n in Definition 3.1. For example, if (10) also had a non-chemical term in the second equation, then the vector fields would have to be multiplied by $x_1 x_2$. See Appendix B and e.g. [11, 12] for more details about this map.

3.2 \mathbf{x} -factorable map

Let us now multiply vector field in the first equation of (10) by x_1 , and that in the second equation by x_2 , thus obtaining CDS

$$\begin{aligned}\frac{dx_1}{dt} &= x_1 \left(-\frac{45}{4} + \frac{1}{8}x_1 + \frac{1}{2}x_2 \right), \\ \frac{dx_2}{dt} &= x_2 \left(\frac{135}{8} + \frac{1}{2}x_1 - \frac{51}{32}x_2 - \frac{1}{20}x_1x_2 + \frac{1}{20}x_2^2 \right).\end{aligned}\tag{15}$$

The map that transforms DS (10) into CDS (15) is called the \mathbf{x} -factorable map [14]. More generally, the \mathbf{x} -factorable map can be applied systematically as follows: multiply the vector field g_i in equation i from (4) by x_i for all $i = 1, 2, \dots, N$. State-space for (15) is shown in Figure 1(e), while a corresponding (t, x_1) -space in Figure 1(f). One can notice that the \mathbf{x} -factorable map has reversed stability of the target equilibrium and destroyed the limit cycle.

In contrast to the failure of the \mathbf{x} -factorable map in Figure 1(e)–(f), a number of examples are presented in [14] indicating that this map can preserve equilibria, limit cycles, and even chaotic attractors; however, no rigorous results are put forward. Instead, the authors from [14] suggest a heuristic: to preserve a dynamical feature in the state-space, this feature should be translated sufficiently far from the axes in the non-negative orthant before the \mathbf{x} -factorable map is applied. Let us stress that this heuristic does not impose any constraints on the direction in which the target feature is translated; it simply demands that the translation is sufficiently large. Let us now prove by counter-example that this heuristic can fail even for hyperbolic equilibria.

Counter-example. Consider a perturbed harmonic oscillator

$$\begin{aligned}\frac{dy_1}{dt} &= \frac{1}{2}y_2 + \frac{25}{2}\varepsilon^2 y_1, \\ \frac{dy_2}{dt} &= -\frac{1}{2}y_1 + \frac{1}{2}\varepsilon(-y_1y_2 + y_2^2) - \frac{75}{8}\varepsilon^2 y_2.\end{aligned}\tag{16}$$

Using e.g. theory from [1][Chapter 4.11], one can show that (16) has an unstable hyperbolic equilibrium at the origin surrounded by a unique stable hyperbolic limit cycle for all $\varepsilon > 0$ sufficiently small. Under translations $x_1 = (y_1 + 10)$, $x_2 = (y_2 + 20)$ and with $\varepsilon = 1/10$, DS (16) becomes (10).

Let us now fix $\varepsilon = 1/10$, translate the variables via $x_1 = (y_1 + 1/\mu)$ and $x_2 = (y_2 + 2/\mu)$ in (16), where $\mu > 0$ is a parameter, and then apply the \mathbf{x} -factorable map, thus obtaining CDS

$$\begin{aligned}\frac{dx_1}{dt} &= x_1 \left[\frac{1}{8} \left(x_1 - \frac{1}{\mu} \right) + \frac{1}{2} \left(x_2 - \frac{2}{\mu} \right) \right], \\ \frac{dx_2}{dt} &= x_2 \left[-\frac{1}{2} \left(x_1 - \frac{1}{\mu} \right) - \frac{1}{20} \left(x_1 - \frac{1}{\mu} \right) \left(x_2 - \frac{2}{\mu} \right) + \frac{1}{20} \left(x_2 - \frac{2}{\mu} \right)^2 - \frac{3}{32} \left(x_2 - \frac{2}{\mu} \right) \right].\end{aligned}\quad (17)$$

Note that (17) reduces to (15) when $\mu = 1/10$. Does the heuristic from [14] hold, i.e. does the equilibrium $(1/\mu, 2/\mu)$ from (17) qualitatively match the unstable equilibrium $(10, 20)$ from (10) if $\mu > 0$ is sufficiently small? Trace of the Jacobian matrix for (17) at $(1/\mu, 2/\mu)$ is given by $-1/(16\mu)$, and the determinant by $61/(128\mu^2)$. Therefore, the equilibrium $(1/\mu, 2/\mu)$ is stable for all $\mu > 0$, i.e. no matter how far it is translated from the boundary of \mathbb{R}_{\geq}^2 . Therefore, the heuristic fails, and the \mathbf{x} -factorable map, not even preserving the hyperbolic equilibrium, is not chemical.

4 Quasi-chemical map: Theory

In Section 3, we have designed CDSs by firstly translating the variables, and then multiplying the vector field with appropriate monomials. In this section, we take a different approach to designing CDSs: we first introduce suitable perturbations to the vector field, and then employ large translations of variables. Let us introduce this new approach with two examples, before presenting general results.

Example. Let us fix $\varepsilon = 1/10$ in DS (16), and perturb its vector field as follows

$$\begin{aligned}\frac{dz_1}{dt} &= \frac{1}{2}z_2 + \frac{1}{8}z_1 + \mu z_1 \left[\frac{1}{2}z_2 + \frac{1}{8}z_1 \right], \\ \frac{dz_2}{dt} &= -\frac{1}{2}z_1 + \frac{1}{20}(-z_1z_2 + z_2^2) - \frac{3}{32}z_2 + \frac{\mu}{2}z_2 \left[-\frac{1}{2}z_1 + \frac{1}{20}(-z_1z_2 + z_2^2) - \frac{3}{32}z_2 \right].\end{aligned}\quad (18)$$

The target equilibrium and limit cycle of (16) are hyperbolic, and therefore robust; see Section 2.1. Hence, there exists $\mu_0 > 0$ such that for all $\mu \in (0, \mu_0)$ DS (18) displays an equilibrium surrounded by a limit cycle that are arbitrarily close and qualitatively equivalent to those of (16).

Let us now exploit the perturbations to make (18) chemical. To this end, we fix $\mu \in (0, \mu_0)$ and translate the variables via $x_1 = (z_1 + 1/\mu)$ and $x_2 = (z_2 + 2/\mu)$, leading to the qualitatively equivalent CDS

$$\begin{aligned}\frac{dx_1}{dt} &= \mu x_1 \left[\frac{1}{2} \left(x_2 - \frac{2}{\mu} \right) + \frac{1}{8} \left(x_1 - \frac{1}{\mu} \right) \right], \\ \frac{dx_2}{dt} &= \frac{\mu}{2} x_2 \left[-\frac{1}{2} \left(x_1 - \frac{1}{\mu} \right) - \frac{1}{20} \left(x_1 - \frac{1}{\mu} \right) \left(x_2 - \frac{2}{\mu} \right) + \frac{1}{20} \left(x_2 - \frac{2}{\mu} \right)^2 - \frac{3}{32} \left(x_2 - \frac{2}{\mu} \right) \right].\end{aligned}\quad (19)$$

Fixing $\mu = 1/10$ in (19), one obtains

$$\begin{aligned}\frac{dx_1}{dt} &= \frac{x_1}{10} \left(-\frac{45}{4} + \frac{1}{8}x_1 + \frac{1}{2}x_2 \right), \\ \frac{dx_2}{dt} &= \frac{x_2}{20} \left(\frac{135}{8} + \frac{1}{2}x_1 - \frac{51}{32}x_2 - \frac{1}{20}x_1x_2 + \frac{1}{20}x_2^2 \right).\end{aligned}\quad (20)$$

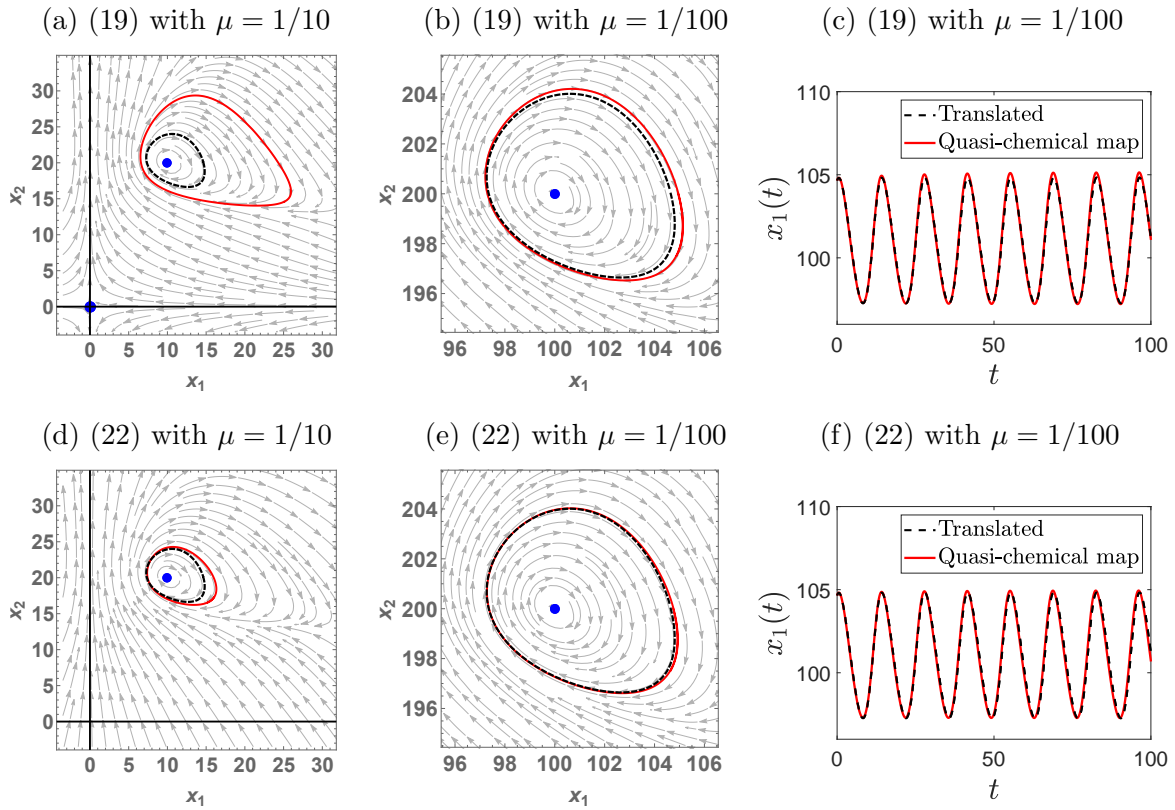


Figure 2: Application of the QCM (24) on DS (16). Panel (a) displays state-space for (19) with $\mu = 1/10$, with the limit cycle shown as the red curve, the equilibrium as the blue dot, and vector field as gray arrows; also shown is the limit cycle of (10) as the black dashed curve. Panel (b) displays a similar plot for (19) with $\mu = 1/100$, while panel (c) shows a corresponding time-state space. Analogous plots are shown in panels (d)–(f) for system (22).

In Figure 2(a), we display state-space for (20), which contains an unstable equilibrium (blue dot) enclosed by a stable limit cycle (red curve), in qualitative agreement with (16) (and, therefore (10)). Note that (20) can be interpreted as a correction, via a suitable rescaling of the vector field, of \mathbf{x} -factorable system (15), which itself fails to qualitatively match the target DS; see Figure 1(e)–(f).

In Figure 2(a), we also show the limit cycle of (10) as dashed black curve, which is in quantitative disagreement with the limit cycle of (20). By design, this mismatch can be made arbitrarily small if $\mu > 0$ is chosen sufficiently small. For example, in Figure 2(b), we display state-space for (19) with $\mu = 1/100$, where one can notice a significantly improved match with the target limit cycle. A corresponding time-state space is shown in Figure 2(c), demonstrating that the period of oscillations is also approximately preserved.

Example. Let us again consider DS (16) with $\varepsilon = 1/10$, and perturb only its first equation:

$$\begin{aligned} \frac{dz_1}{dt} &= \frac{1}{2}z_2 + \frac{1}{8}z_1 + \mu z_1 \left[\frac{1}{2}z_2 + \frac{1}{8}z_1 \right], \\ \frac{dz_2}{dt} &= -\frac{1}{2}z_1 + \frac{1}{20}(-z_1z_2 + z_2^2) - \frac{3}{32}z_2. \end{aligned} \quad (21)$$

Translating the variables according to $x_1 = (z_1 + 1/\mu)$ and $x_2 = (z_2 + 2/\mu)$, one obtains the qualitatively equivalent system

$$\begin{aligned} \frac{dx_1}{dt} &= \mu x_1 \left[\frac{1}{2} \left(x_2 - \frac{2}{\mu} \right) + \frac{1}{8} \left(x_1 - \frac{1}{\mu} \right) \right], \\ \frac{dx_2}{dt} &= -\frac{1}{2} \left(x_1 - \frac{1}{\mu} \right) - \frac{1}{20} \left(x_1 - \frac{1}{\mu} \right) \left(x_2 - \frac{2}{\mu} \right) + \frac{1}{20} \left(x_2 - \frac{2}{\mu} \right)^2 - \frac{3}{32} \left(x_2 - \frac{2}{\mu} \right). \end{aligned} \quad (22)$$

One can readily show that the vector field in the second equation is chemical for all sufficiently small $\mu > 0$, making (22) chemical then. Fixing $\mu = 1/10$ in (22), one obtains CDS

$$\begin{aligned}\frac{dx_1}{dt} &= \frac{x_1}{10} \left(-\frac{45}{4} + \frac{1}{8}x_1 + \frac{1}{2}x_2 \right), \\ \frac{dx_2}{dt} &= \frac{135}{8} + \frac{1}{2}x_1 - \frac{51}{32}x_2 - \frac{1}{20}x_1x_2 + \frac{1}{20}x_2^2.\end{aligned}\tag{23}$$

In Figure 2(d), we display state-space of (23), showing an unstable equilibrium and a stable limit cycle which are in qualitative agreement with (10). Figure 2(e)–(f) displays state and time-state spaces for (22) when $\mu = 1/100$, showing an excellent match with the target DS. Let us emphasize an important difference between (19) and (22): the former is cubic, while the latter is *quadratic*.

Quasi-chemical map. Let us now formalize the map underlying (19) and (22).

Definition 4.1. (*Quasi-chemical map*) Consider DS (1). Consider also

$$\frac{dx_i}{dt} = q_i \left(\mathbf{x} - \frac{\mathbf{T}}{\mu} \right) + \frac{\mu}{T_i} x_i \left[f_i \left(\mathbf{x} - \frac{\mathbf{T}}{\mu} \right) - q_i \left(\mathbf{x} - \frac{\mathbf{T}}{\mu} \right) \right], \quad i = 1, 2, \dots, N,\tag{24}$$

where $\mathbf{T} = (T_1, T_2, \dots, T_N)^\top \in \mathbb{R}_{>}^N$ is a fixed vector, $\mu > 0$ is a free parameter, and $q_i(\mathbf{x} - \mathbf{T}/\mu) \in \mathbb{P}_n^{\mathcal{C}}(\mathbb{R}^N, \mathbb{R})$ are arbitrary polynomials of degree at most n that are chemical for all sufficiently small $\mu > 0$ and for all $i = 1, 2, \dots, N$; we say that $q_i(\mathbf{x})$ are quasi-chemical. Then, $\Psi_\mu : \mathbb{P}_n(\mathbb{R}^N, \mathbb{R}^N) \rightarrow \mathbb{P}_{n+1}^{\mathcal{C}}(\mathbb{R}^N, \mathbb{R}^N)$, mapping the vector field of DS (1) to the vector field of CDS (24) for all sufficiently small $\mu > 0$, is called a quasi-chemical map (QCM).

Remark. In Definition 4.1, we assume that $T_i > 0$. If $T_i = 0$, then we define $dx_i/dt = f_i(\mathbf{x} - \mathbf{T}/\mu)$ in (24), under the additional assumption that $f_i(\mathbf{x} - \mathbf{T}/\mu)$ with $T_i = 0$ is quasi-chemical.

Remark. In Appendix C, we present a more general definition of the QCM.

The following fundamental lemma is readily provable.

Lemma 4.1. Under the translation of variables $z_i = (x_i - T_i/\mu)$ for every $\mu > 0$, DS (24) becomes

$$\frac{dz_i}{dt} = f_i(\mathbf{z}) + \mu \frac{z_i}{T_i} [f_i(\mathbf{z}) - q_i(\mathbf{z})], \quad i = 1, 2, \dots, N.\tag{25}$$

Lemma 4.1 shows that the QCM essentially just perturbs the target DS (1), which allows us to apply the theory of regular perturbations to deduce a number of results. We start by showing that the QCM is a chemical one when it comes to preserving robust regions in state-space. To this end, for any set $\mathbb{U} \subset \mathbb{R}^N$ and vector $\mathbf{T} \in \mathbb{R}^N$, we let $\mathbb{U} + \mathbf{T} = \{\mathbf{x} + \mathbf{T} \in \mathbb{R}^N \mid \mathbf{x} \in \mathbb{U}\}$.

Theorem 4.1. (QCM) Assume that DS (1) is robust in compact set $\mathbb{U} \subset \mathbb{R}^N$. Then, for every sufficiently small $\mu > 0$, CDS (24) in $\mathbb{U} + \mathbf{T}/\mu \subset \mathbb{R}_{>}^N$ is qualitatively equivalent to DS (1) in \mathbb{U} .

Proof. The perturbation from (25) is given by $(\mathbf{F}(\mathbf{z}; \mu))_i = \mu(z_i/T_i)[f_i(\mathbf{z}) - q_i(\mathbf{z})]$, and satisfies $\mathbf{F} \in C^1$ and $\mathbf{F}(\mathbf{z}; 0) = \mathbf{0}$. Hence, using the assumption that (1) is robust in \mathbb{U} , Definition 2.1 implies existence of $\mu_0 > 0$ such that (25) and (1) are qualitatively equivalent in \mathbb{U} for every $\mu \in (0, \mu_0)$. By Lemma 4.1, system (24) in $\mathbb{U} + \mathbf{T}/\mu$ is qualitatively equivalent to (25) in \mathbb{U} for every $\mu > 0$. Hence, (24) in $\mathbb{U} + \mathbf{T}/\mu \subset \mathbb{R}_{>}^N$ is also qualitatively equivalent to (1) in \mathbb{U} for every $\mu \in (0, \mu_0)$. \square

Remark. In Theorem 4.1, we have assumed that DS (1) is robust, i.e. remains qualitatively equivalent in \mathbb{U} under *every* continuously differentiable perturbation, as per Definition 2.1. However, the proof shows that Theorem 4.1 holds under a much less strict assumption: it is only required that (1)

remains qualitatively equivalent in \mathbb{U} under the *special* $(n + 1)$ -degree polynomial perturbations $(\mathbf{F}(\mathbf{z}; \mu))_i = \mu(z_i/T_i)[f_i(\mathbf{z}) - q_i(\mathbf{z})]$ from (25), which we call *chemical perturbations*.

Theorem 4.1 holds under any choice of the quasi-chemical functions q_i in (24). Let us now re-state this theorem under a special choice of q_i .

Theorem 4.2. *Assume that N -dimensional n -degree DS (1) is robust in $\mathbb{U} \subset \mathbb{R}^N$. Then, for every sufficiently small $\mu > 0$, N -dimensional $(n + 1)$ -degree CDS*

$$\frac{dx_i}{dt} = \frac{\mu}{T_i} x_i f_i \left(\mathbf{x} - \frac{\mathbf{T}}{\mu} \right), \quad i = 1, 2, \dots, N, \quad (26)$$

in $\mathbb{U} + \mathbf{T}/\mu \subset \mathbb{R}_{\geq}^N$ is qualitatively equivalent to DS (1) in \mathbb{U} .

Proof. Fixing the quasi-chemical function $q_i = 0$ for $i = 1, 2, \dots, N$ in (24) yields (26). The statement of the theorem then follows from Theorem 4.1. \square

Remark. Theorem 4.2 shows that the \mathbf{x} -factorable map [14] qualitatively preserves robust features if they are translated uniformly, $T_1 = T_2 = \dots = T_N$, i.e. the direction of translation is important; however, even in this case, time is distorted.

4.1 Quantitative properties

In this section, we augment Theorem 4.1 with more precise, *quantitative*, results for some special robust solutions, namely solutions over finite time-intervals, hyperbolic equilibria and hyperbolic limit cycles. For more complicated solutions, quantitative results are more difficult to obtain; in such cases, trapping regions can be useful (see Appendix A). In what follows, we write $\mathbf{x}(\mu) = \mathbf{y} + \mathcal{O}(\mu)$ if $\|\mathbf{x}(\mu) - \mathbf{y}\| \leq c\mu$ for all sufficiently small $\mu > 0$, where $c > 0$ is a μ -independent constant.

Theorem 4.3. (QCM: Quantitative properties)

- (i) **Finite time-intervals.** *Let $\mathbf{y}(t) = \mathbf{y}(t; \mathbf{y}_0)$ be a solution of (1) for all $t \in [0, t_0]$ for some finite $t_0 > 0$. Then, for all sufficiently small μ (24) has a unique solution $\mathbf{x}(t; \mu) = \mathbf{x}(t; \mu, \mathbf{y}_0 + \mathbf{T}/\mu)$ for all $t \in [0, t_0]$. Furthermore, $\mathbf{x}(t; \mu) = (\mathbf{y}(t) + \mathbf{T}/\mu) + \mathcal{O}(\mu)$ uniformly for $t \in [0, t_0]$.*
- (ii) **Equilibria.** *Let \mathbf{y}^* be a hyperbolic equilibrium of (1). Then, for all sufficiently small μ (24) has a unique hyperbolic equilibrium $\mathbf{x}^*(\mu)$ in a neighborhood of $(\mathbf{y}^* + \mathbf{T}/\mu)$. In particular, $\mathbf{x}^*(\mu) = (\mathbf{y}^* + \mathbf{T}/\mu) + \mathcal{O}(\mu)$. Equilibrium $\mathbf{x}^*(\mu)$ is qualitatively equivalent to \mathbf{y}^* . In particular, eigenvalues $\lambda_{1,\mu}, \dots, \lambda_{N,\mu}$ associated to $\mathbf{x}^*(\mu)$ can be ordered so that $\lim_{\mu \rightarrow 0} \lambda_{i,\mu} = \lambda_{i,0}$ for all $i = 1, \dots, N$, where $\lambda_{1,0}, \dots, \lambda_{N,0}$ are the eigenvalues associated to \mathbf{y}^* .*
- (iii) **Limit cycles.** *Let \mathbf{y}_{τ_0} be a hyperbolic limit cycle of (1) with period $\tau_0 > 0$. Then, for all sufficiently small μ (24) has a unique hyperbolic limit cycle \mathbf{x}_{τ_μ} with period $\tau_\mu > 0$ in a neighborhood of $(\mathbf{y}_{\tau_0} + \mathbf{T}/\mu)$. In particular, $\mathbf{x}_{\tau_\mu}(t) = (\mathbf{y}_{\tau_0}(t) + \mathbf{T}/\mu) + \mathcal{O}(\mu)$ uniformly over finite time-intervals, and $\tau_\mu = \tau_0 + \mathcal{O}(\mu)$. Limit cycle \mathbf{x}_{τ_μ} is qualitatively equivalent to \mathbf{y}_{τ_0} . In particular, characteristic exponents $\rho_{1,\mu}, \dots, \rho_{N,\mu}$ associated to \mathbf{x}_{τ_μ} can be ordered so that $\lim_{\mu \rightarrow 0} \rho_{i,\mu} = \rho_{i,0}$ for all $i = 1, \dots, N$, where $\rho_{1,0}, \dots, \rho_{N,0}$ are the characteristic exponents associated to \mathbf{y}_{τ_0} .*
- (iv) **Trapping regions.** *Let $\mathbb{S}_0 = \{\mathbf{y} \in \mathbb{R}^N | V(\mathbf{y}) \leq r \text{ for some } r > 0\}$ be a trapping region for (1). Then, $\mathbb{S}_\mu = \{\mathbf{x} \in \mathbb{R}^N | V(\mathbf{x} - \mathbf{T}/\mu) \leq r\}$ is a trapping region for (24) for all sufficiently small $\mu > 0$.*

Proof. To prove statement (i), we use the fact that, if $\mathbf{y}(t) = \mathbf{y}(t; \mathbf{y}_0)$ is a solution of (1) for all $t \in [0, t_0]$, then for all sufficiently small $\mu > 0$ system (25) has a unique solution $\mathbf{z}(t; \mu) = \mathbf{z}(t; \mu, \mathbf{y}_0)$ for all $t \in [0, t_0]$, and $\mathbf{z}(t; \mu) = \mathbf{y}(t) + \mathcal{O}(\mu)$ uniformly for $t \in [0, t_0]$ [17][Chapter 1]. Statement (i) then follows from Lemma 4.1 via the translation of variables $\mathbf{x} = \mathbf{z} + \mathbf{T}/\mu$. Statements (ii) and (iii) are proved analogously, using e.g. the theory from [17][Chapter 14]. To prove statement (iv), we use Definition A.5 to deduce that $\mathbf{f}(\mathbf{y}) \cdot \mathbf{n}(\mathbf{y}) < 0$ for all $\mathbf{y} \in \mathbb{R}^N$ on the boundary $V(\mathbf{y}) = r$ with outward-pointing normal $\mathbf{n}(\mathbf{y}) \in \mathbb{R}^N$, where \cdot denotes the dot product. Therefore, the vector field of (25) satisfies $\mathbf{f}(\mathbf{z}) \cdot \mathbf{n}(\mathbf{z}) + \mathcal{O}(\mu) < 0$ on the boundary $V(\mathbf{z}) = r$ for every $\mu > 0$ sufficiently small; hence, \mathbb{S}_0 is also a trapping region for (25). Statement (iv) then follows from Lemma 4.1. \square

Theorem 4.3(i) shows that the corresponding solutions of CDS (24) and target DS (1) stay, up to a translation, within $\mathcal{O}(\mu)$ -distance for any finite time-interval. This alignment of trajectories holds without a time re-scaling, i.e. the QCM approximately preserves the time-scale (time-parametrization) along the solutions; this is in contrast to the time-change map from Section 3. Theorem 4.3(ii) shows that the corresponding hyperbolic equilibria of (24) and (1) are also within $\mathcal{O}(\mu)$ -distance. Furthermore, the corresponding eigenvalues are arbitrarily close; consequently, the QCM preserves, not only stability, but also the type of hyperbolic equilibria. Analogous conclusions are reached for hyperbolic limit cycles in Theorem 4.3(iii); in addition, the periods of oscillations of the corresponding limit cycles are $\mathcal{O}(\mu)$ -close. Finally, Theorem 4.3(iv) shows that the QCM preserves trapping regions.

4.2 Bifurcations

Theorem 4.1 is applicable when the target DS (2) is robust in $\mathbb{U} \subset \mathbb{R}^N$. In this section, we consider the case when (2) is not robust in \mathbb{U} . To this end, we now explicitly display dependence of vector fields on some parameters, which we always assume is continuously differentiable. In particular, to indicate dependence of (2) on some parameters $\boldsymbol{\beta} \in \mathbb{R}^P$, we write

$$\frac{d\mathbf{y}}{dt} = \mathbf{f}(\mathbf{y}; \boldsymbol{\beta}), \quad \text{where } \mathbf{f}(\mathbf{y}; \cdot) \in C^1(\mathbb{R}^P, \mathbb{R}^N). \quad (27)$$

Consider also the perturbed DS (3), written as

$$\frac{d\mathbf{z}}{dt} = \mathbf{f}(\mathbf{z}; \boldsymbol{\beta}) + \mathbf{F}(\mathbf{z}; \boldsymbol{\beta}, \mu), \quad \text{where } \mathbf{F} \in C^1(\mathbb{R}^N \times \mathbb{R}^P \times \mathbb{R}_{\geq}, \mathbb{R}^N) \text{ and } \mathbf{F}(\mathbf{z}; \boldsymbol{\beta}, 0) = \mathbf{0}. \quad (28)$$

Let us fix the parameters to $\boldsymbol{\beta} = \boldsymbol{\beta}^* \in \mathbb{R}^P$, and assume that then (27) is not robust in compact set $\mathbb{U} \subset \mathbb{R}^N$. This means that, for some perturbations \mathbf{F} , DSs (28) and (27) at $\boldsymbol{\beta} = \boldsymbol{\beta}^*$ are qualitatively different in \mathbb{U} , and (27) is said to undergo a *bifurcation* [1, 15]. Even though (28) at $\boldsymbol{\beta} = \boldsymbol{\beta}^*$ is in general qualitatively different from (27) at $\boldsymbol{\beta} = \boldsymbol{\beta}^*$, (28) at a slightly different parameter value, say $\boldsymbol{\beta} = \boldsymbol{\beta}^{**} \in \mathbb{R}^P$, may be qualitatively equivalent to (27) at $\boldsymbol{\beta} = \boldsymbol{\beta}^*$. In this case, we say that the underlying bifurcation is robust.

Definition 4.2. (Robust bifurcation) Assume that DS (27) at $\boldsymbol{\beta} = \boldsymbol{\beta}^* \in \mathbb{R}^P$ is not robust and undergoes a bifurcation \mathcal{B} in $\mathbb{U} \subset \mathbb{R}^N$. Assume furthermore that for every $\varepsilon > 0$, and for every $\mathbf{F} \in C^1$ with $\mathbf{F}(\mathbf{z}; \boldsymbol{\beta}, 0) = \mathbf{0}$, there exists $\mu_0 > 0$ such that for every $\mu \in (0, \mu_0)$ there exists $\boldsymbol{\beta}^{**} \in \mathbb{R}^P$, with $\|\boldsymbol{\beta}^{**} - \boldsymbol{\beta}^*\| < \varepsilon$, such that (28) at $\boldsymbol{\beta} = \boldsymbol{\beta}^{**}$ and (27) at $\boldsymbol{\beta} = \boldsymbol{\beta}^*$ are qualitatively equivalent in \mathbb{U} . Then, DS (27) is said to undergo at $\boldsymbol{\beta} = \boldsymbol{\beta}^*$ a robust bifurcation \mathcal{B} in \mathbb{U} .

We now show that the QCM preserves robust bifurcations.

Theorem 4.4. (QCM: Bifurcations) *Assume that DS (27) at $\beta = \beta^* \in \mathbb{R}^P$ undergoes a robust bifurcation \mathcal{B} in $\mathbb{U} \subset \mathbb{R}^N$. Then, for every sufficiently small $\mu > 0$ there exists $\beta^{**} \in \mathbb{R}^P$, arbitrarily close to β^* , such that CDS (24) at $\beta = \beta^{**}$ undergoes bifurcation \mathcal{B} in $\mathbb{U} + \mathbf{T}/\mu \subset \mathbb{R}_{\geq}^N$.*

Proof. The perturbation from (25) is given by $(\mathbf{F}(\mathbf{z}; \beta, \mu))_i = \mu(z_i/T_i)[f_i(\mathbf{z}; \beta) - q_i(\mathbf{z}; \beta)]$, and satisfies $\mathbf{F} \in C^1$ and $\mathbf{F}(\mathbf{z}; \beta, 0) = \mathbf{0}$. Therefore, using the assumption that (27) at $\beta = \beta^*$ undergoes robust bifurcation \mathcal{B} in $\mathbb{U} \subset \mathbb{R}^N$, Definition 4.2 implies that for every $\varepsilon > 0$ there exists $\mu_0 > 0$ such that for all $\mu \in (0, \mu_0)$ there exists $\beta^{**} \in \mathbb{R}^P$, with $\|\beta^{**} - \beta^*\| < \varepsilon$, such that (25) at $\beta = \beta^{**}$ undergoes bifurcation \mathcal{B} in $\mathbb{U} \subset \mathbb{R}^N$. Since bifurcations are preserved under translations of dependent variables, statement of the theorem then follows from Lemma 4.1. \square

Remark. Analogous to Theorem 4.1, Theorem 4.4 holds for all bifurcations that are robust with respect to the chemical perturbations; robustness with respect to other types of perturbations is irrelevant for the theorem.

5 Quasi-chemical map: Applications

In this section, we use the results from Section 4 to transform some DSs with desired dynamics to CDSs. These tasks could simply be performed by using the special QCM (26). However, in what follows, we instead focus on the more general QCM (24), which has a key advantage: the quasi-chemical functions q_i may be chosen to reduce the number of higher-degree terms in the resulting CDSs, or even preserve the degree of the target DSs. We state most of the results in this section in terms of CRNs; see Appendix A for more details on how to construct CRNs for a given CDS.

5.1 CRN with arbitrary many limit cycles

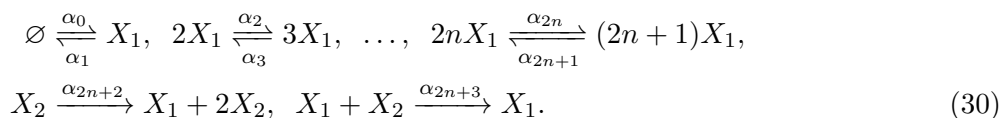
Let us consider the two-dimensional DS

$$\begin{aligned} \frac{dy_1}{dt} &= y_2 + \varepsilon(\beta_0 y_1 + \beta_1 y_1^3 + \dots + \beta_n y_1^{2n+1}), \\ \frac{dy_2}{dt} &= -y_1. \end{aligned} \tag{29}$$

Under a suitable choice of parameters $\beta_0, \beta_1, \dots, \beta_n$, and for all $\varepsilon > 0$ sufficiently small, (29) has n nested hyperbolic limit cycles [18, 1]. We also prove this fact, and provide explicit expressions for a suitable parameter choice, in Appendix D. We now map DS (29) into a CDS of the same degree.

To this end, we denote two irreversible reactions $nX \xrightarrow{\alpha} mX$ and $mX \xrightarrow{\beta} nX$ as a single reversible reaction $nX \xrightleftharpoons[\beta]{\alpha} mX$.

Theorem 5.1. (CRN with arbitrary many limit cycles) *Consider the CRN*



Let $0 < r_1 < r_2 < \dots < r_n$ be arbitrary real numbers. Then, there exist coefficients $\alpha_i = \alpha_i(r_1, r_2, \dots, r_n)$ for $i = 0, 1, \dots, 2N + 3$ such that CRN (30) has n nested hyperbolic limit cycles. The i th limit cycle is arbitrarily close to a circle of radius r_i , and has period arbitrarily close to 2π . The n th limit cycle is stable, and the limit cycles alternate in stability.

Proof. Let us fix $\varepsilon > 0$ to a sufficiently small value, and $\beta_0, \beta_1, \dots, \beta_n$ according to (56) from Appendix D. It then follows from Lemma D.1 that (29) has n nested hyperbolic limit cycles; the i th limit cycle is arbitrarily close to the 2π -periodic circle of radius r_i centered at the origin. Furthermore, the n th limit cycle is stable, and the limit cycles alternative in stability.

Let us apply on (29) the QCM (24) with $T_1 = T_2 = 1$, $q_1 = f_1$ and $q_2 = 0$, leading to

$$\begin{aligned} \frac{dx_1}{dt} &= \left(x_2 - \frac{1}{\mu}\right) + \varepsilon \sum_{i=0}^n \beta_i \left(x_1 - \frac{1}{\mu}\right)^{2i+1} = \sum_{i=0}^{2n+1} (-1)^i \alpha_i x_1^i + \alpha_{2n+2} x_2, \\ \frac{dx_2}{dt} &= -\mu x_2 \left(x_1 - \frac{1}{\mu}\right) = \alpha_{2n+2} x_2 - \alpha_{2n+3} x_1 x_2, \end{aligned} \quad (31)$$

where the coefficients $\alpha_0, \alpha_1, \dots, \alpha_{2n+3}$, are stated explicitly as (57) in Appendix D. Since $\beta_n < 0$, the zero-degree term in the first equation from (31) is dominated by $1/\mu^{2n+1} > 0$ for all sufficiently small $\mu > 0$; therefore, (31) is then a CDS. A CRN induced by (31) is given by (30); see Definition A.6. In particular, we fuse $X_2 \xrightarrow{1} X_1 + X_2$ and $X_2 \xrightarrow{1} 2X_2$ into $X_2 \xrightarrow{1} X_1 + 2X_2$, as per Definition A.7. Statement of the theorem then follows from Theorem 4.3(iii). \square

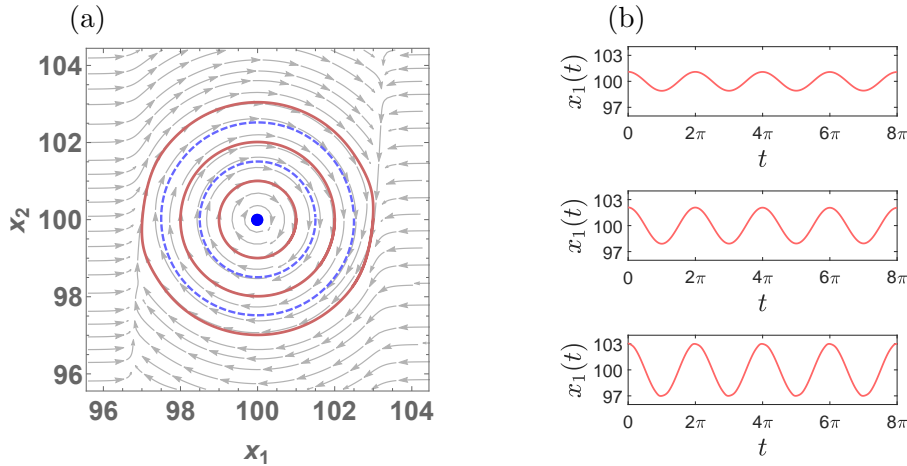
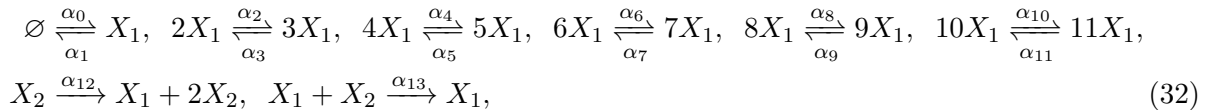


Figure 3: CDS with arbitrary many limit cycles. *Panel (a) displays state-space for CDS (33), corresponding to the CRN (32), with parameters (34), $\varepsilon = 10^{-4}$ and $\mu = 10^{-2}$. The three stable and two unstable limit cycles are respectively shown as solid red and dashed blue curves, and the enclosed equilibrium as the blue dot. Each of the three stable limit cycles is shown in time-state space in one of the sub-panels of panel (b).*

Example. Consider the CRN (30) with $n = 5$:



with the CDS (31) given by

$$\begin{aligned} \frac{dx_1}{dt} &= \left(x_2 - \frac{1}{\mu}\right) + \varepsilon \sum_{i=0}^5 \beta_i \left(x_1 - \frac{1}{\mu}\right)^{2i+1}, \\ \frac{dx_2}{dt} &= -\mu x_2 \left(x_1 - \frac{1}{\mu}\right). \end{aligned} \quad (33)$$

Let us impose that (33) has 5 limit cycles, close to circles with radii $r_1 = 1$, $r_2 = 3/2$, $r_3 = 2$, $r_4 = 5/2$ and $r_5 = 3$. Then, suitable coefficients $\beta_0, \beta_1, \dots, \beta_5$ are given

$$\beta_0 = \frac{2025}{4}, \quad \beta_1 = -\frac{5307}{4}, \quad \beta_2 = 1039, \quad \beta_3 = -\frac{11652}{35}, \quad \beta_4 = \frac{320}{7}, \quad \beta_5 = -\frac{512}{231}. \quad (34)$$

Coefficients (34) can be obtained directly from (56) in Appendix D; alternatively, one can indirectly impose that a suitable polynomial has the desired radii as roots, see (55) in Appendix D. In Figure 3(a), we display state-space for CDS (33) with parameters (34), $\varepsilon = 10^{-4}$ and $\mu = 10^{-2}$. As desired, the system has three stable limit cycles, shown as red solid curves, and two unstable ones, shown as dashed blue curves, all of which are approximately circular. In Figure 3(b), we show three sub-panels, each displaying one of the stable limit cycles in time-state space; one can notice that each of the limit cycles is approximately 2π -periodic.

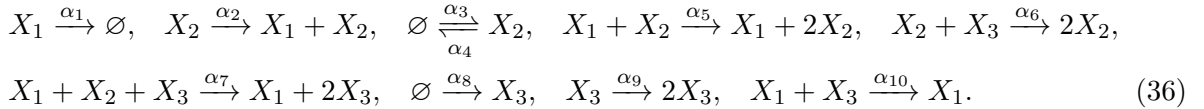
5.2 CRN with chaos

In this section, we design a CDS whose long-time dynamics is neither an equilibrium nor a limit cycle. To this end, let us consider the Lorenz system [19]:

$$\begin{aligned} \frac{dy_1}{dt} &= -10y_1 + 10y_2, \\ \frac{dy_2}{dt} &= 28y_1 - y_2 - y_1y_3, \\ \frac{dy_3}{dt} &= -\frac{8}{3}y_3 + y_1y_2. \end{aligned} \quad (35)$$

In Figure 4(a), we show the butterfly-like chaotic attractor of (35), called the Lorenz attractor, projected into (y_1, y_3) -space, while a corresponding (t, y_1) -space is shown in Figure 4(b).

Theorem 5.2. (CRN with Lorenz attractor) *Consider the CRN*



Assume that the rate coefficients are given by

$$\begin{aligned} \alpha_1 = 10, \quad \alpha_2 = 10, \quad \alpha_3 = \frac{1}{\mu}, \quad \alpha_4 = \frac{1}{\mu} + 29, \quad \alpha_5 = 1 + 28\mu, \quad \alpha_6 = 1, \\ \alpha_7 = \mu, \quad \alpha_8 = \frac{8}{3\mu}, \quad \alpha_9 = \frac{1}{\mu} - \frac{8}{3}, \quad \alpha_{10} = 1. \end{aligned} \quad (37)$$

Then, for every sufficiently small $\mu > 0$, CRN (36) has a chaotic attractor that is qualitatively equivalent to the Lorenz attractor.

Proof. Let us apply on (35) the QCM (24) with $T_1 = T_2 = T_3 = 1$, $q_1 = f_1$, $q_2 = -y_2$ and $q_3 = -(8/3)y_3$, leading to

$$\begin{aligned} \frac{dx_1}{dt} &= -10x_1 + 10x_2, \\ \frac{dx_2}{dt} &= -\left(x_2 - \frac{1}{\mu}\right) + \mu x_2 \left[28 \left(x_1 - \frac{1}{\mu}\right) - \left(x_1 - \frac{1}{\mu}\right) \left(x_3 - \frac{1}{\mu}\right) \right], \\ \frac{dx_3}{dt} &= -\frac{8}{3} \left(x_3 - \frac{1}{\mu}\right) + \mu x_3 \left[\left(x_1 - \frac{1}{\mu}\right) \left(x_2 - \frac{T}{\mu}\right) \right]. \end{aligned} \quad (38)$$

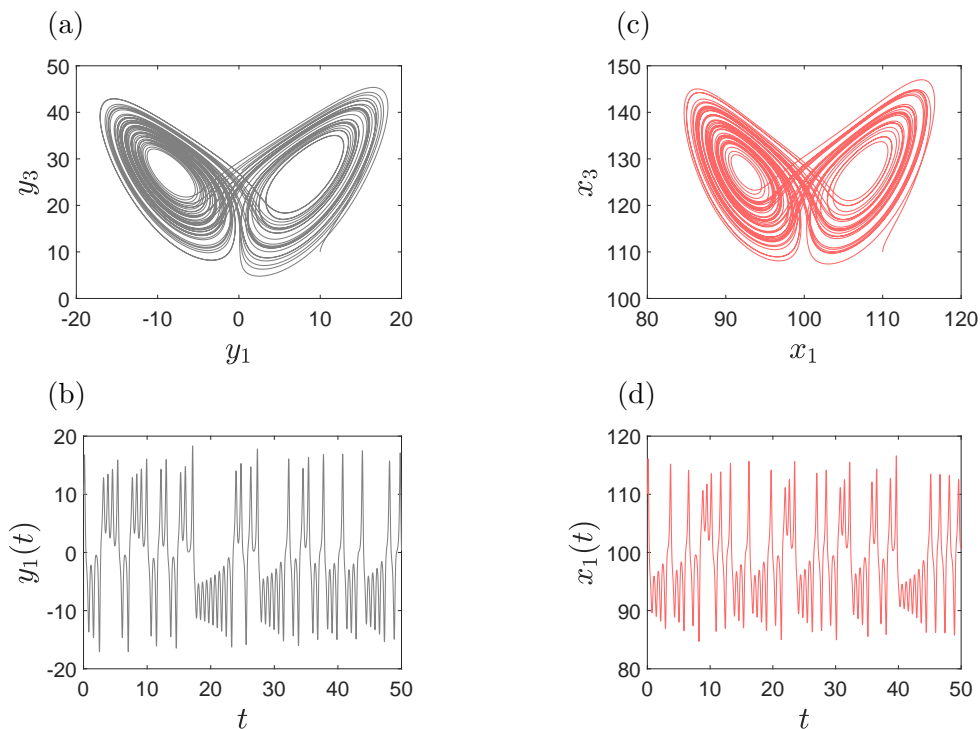


Figure 4: CDS with Lorenz attractor. *Panels (a) and (b) respectively display (y_1, y_3) - and (t, y_1) -space for the Lorenz system (35) with initial condition $y_1(0) = y_2(0) = y_3(0) = 10$. Analogous plots are shown in panels (c) and (d) for CDS (39) with initial condition $x_1(0) = x_2(0) = x_3(0) = 10 + 100$.*

DS (38) is chemical for all $\mu > 0$, and induces CRN (36) with coefficients (37). Using the fact that Lorenz attractor is robust [20], the statement of the theorem follows from Theorem 4.1. \square

Let us fix $\mu = 1/100$ in (37); the CDS (38) induced by (36) then reads

$$\begin{aligned}
 \frac{dx_1}{dt} &= -10x_1 + 10x_2, \\
 \frac{dx_2}{dt} &= 100 - 129x_2 + \frac{32}{25}x_1x_2 + x_2x_3 - \frac{1}{100}x_1x_2x_3, \\
 \frac{dx_3}{dt} &= \frac{800}{3} + \frac{292}{3}x_3 - x_1x_3 - x_2x_3 + \frac{1}{100}x_1x_2x_3.
 \end{aligned} \tag{39}$$

State-space and time-state space for (39) are respectively shown in Figure 4(c) and (d), which compare well with Figure 4(a)–(b). Note that Lorenz system (35) and its chemical counterpart (39) evolve on a similar time-scale, consistent with Theorem 4.3(i). Note also that, while Lorenz attractor itself is robust with respect to perturbations, the underlying trajectories in the time-state space are sensitive; for this reason, the two trajectories from Figures 4(b) and (d) differ after some time.

Chemical Lorenz system (39) is cubic. In Appendix E, we present a candidate chaotic CDS which is quadratic.

5.3 CRN with homoclinic bifurcation

Consider the two-dimensional DS

$$\begin{aligned}\frac{dy_1}{dt} &= \left(\beta - \frac{4}{5}\right)y_1 + y_2 - \frac{6}{5}y_1y_2 + \frac{3}{2}y_2^2, \\ \frac{dy_2}{dt} &= y_1 - \frac{4}{5}y_2 - \frac{4}{5}y_2^2,\end{aligned}\tag{40}$$

which undergoes a super-critical homoclinic bifurcation [21, 6]. In particular, when $\beta = 0$, DS (40) has a saddle equilibrium at the origin, whose stable and unstable manifolds connect, forming a tear-shaped homoclinic loop; see Figure 5(b), where we also display an unstable focus inside the homoclinic loop, and a stable node in the first quadrant. While the saddle is robust, the homoclinic loop is not - when β is slightly varied, the saddle manifolds do not connect, and a bifurcation occurs. More precisely, when $\beta < 0$, the unstable manifold of the saddle “undershoots” and forms a stable limit cycle around the focus, as shown in Figure 5(a). On the other hand, when $\beta > 0$, the unstable manifold “overshoots”, and is connected to the stable node, see Figure 5(c).

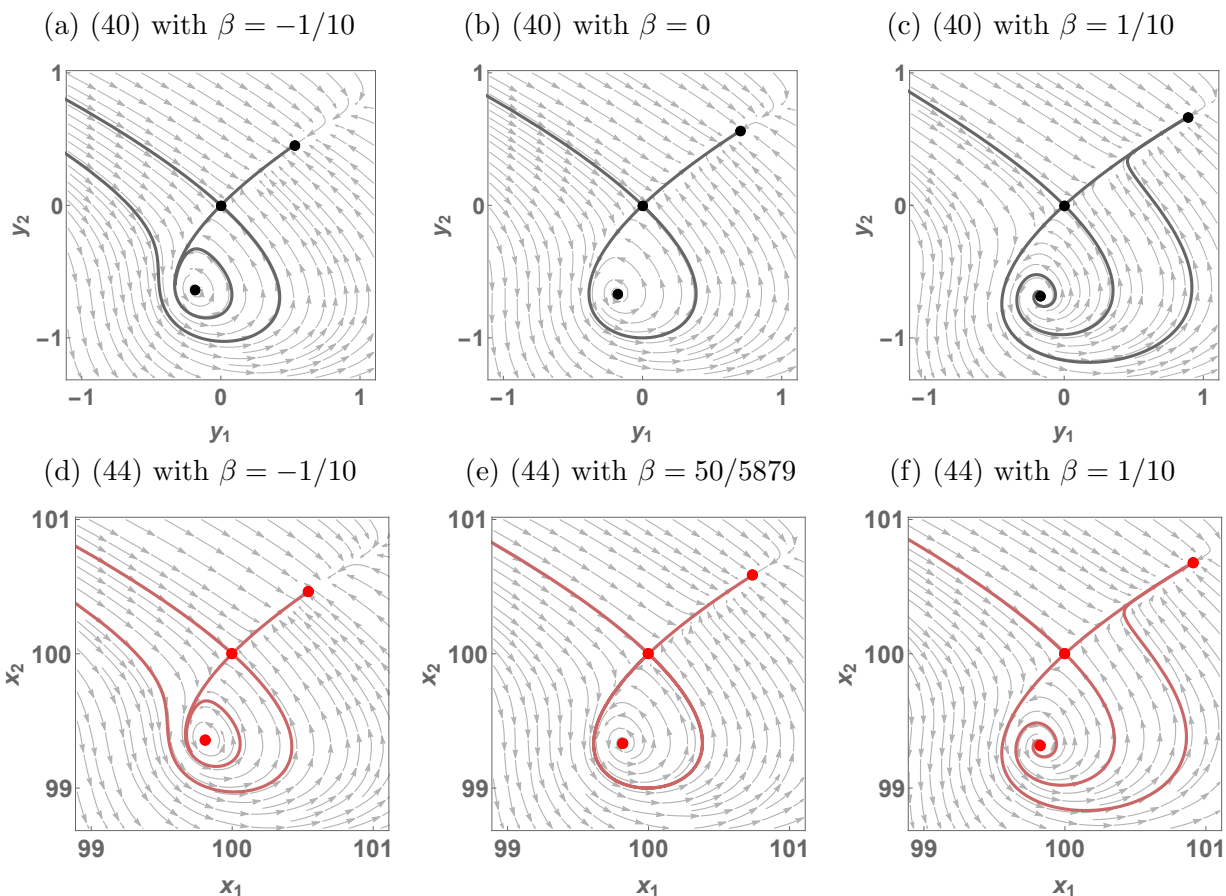
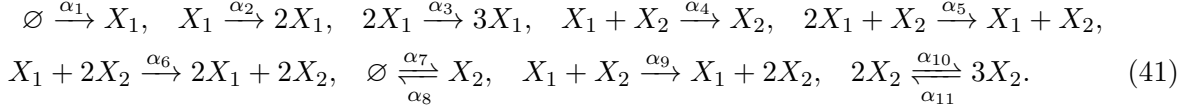


Figure 5: CDS undergoing homoclinic bifurcation. *Panels (a)–(c) display state-space for DS (40) for three different values of β , where at $\beta = 0$ a homoclinic bifurcation takes place. Analogous plots are shown for CDS (44) in panels (d)–(f).*

Theorem 5.3. (CRN with homoclinic bifurcation) Consider the CRN



Assume that the rate coefficients are given by

$$\begin{aligned} \alpha_1 &= \frac{4}{5\mu} - \frac{\beta}{\mu}, & \alpha_2 &= \frac{3}{10\mu} - \frac{9}{5} + \beta, & \alpha_3 &= \frac{6}{5}, & \alpha_4 &= \frac{9}{5} - \mu, & \alpha_5 &= \frac{6}{5}\mu, \\ \alpha_6 &= \frac{3}{2}\mu, & \alpha_7 &= \frac{4}{5\mu}, & \alpha_8 &= \frac{4}{5\mu} + \frac{9}{5}, & \alpha_9 &= \mu, & \alpha_{10} &= \frac{8}{5}, & \alpha_{11} &= \frac{4}{5}\mu. \end{aligned} \quad (42)$$

Then, for every sufficiently small $\mu > 0$, CRN (41) undergoes a super-critical homoclinic bifurcation at saddle $(1/\mu, 1/\mu) \in \mathbb{R}_>^2$ at some parameter value $\beta = \beta(\mu)$ arbitrarily close to zero.

Proof. Let us apply on (40) the QCM (24) with $T_1 = T_2 = 1$, $q_1 = (\beta - 4/5)y_1$ and $q_2 = -(4/5)y_2$, leading to the DS

$$\begin{aligned} \frac{dx_1}{dt} &= \left(\beta - \frac{4}{5}\right) \left(x_1 - \frac{1}{\mu}\right) + \mu x_1 \left[\left(x_2 - \frac{1}{\mu}\right) - \frac{6}{5} \left(x_1 - \frac{1}{\mu}\right) \left(x_2 - \frac{1}{\mu}\right) + \frac{3}{2} \left(x_2 - \frac{1}{\mu}\right)^2 \right], \\ \frac{dx_2}{dt} &= -\frac{4}{5} \left(x_2 - \frac{1}{\mu}\right) + \mu x_2 \left[\left(x_1 - \frac{1}{\mu}\right) - \frac{4}{5} \left(x_2 - \frac{1}{\mu}\right)^2 \right], \end{aligned} \quad (43)$$

which is chemical for every $\beta \leq 4/5$, and for every $\mu > 0$; an induced CRN is given by (41) with coefficients (42). DS (40) at $\beta = 0$ undergoes a super-critical homoclinic bifurcation which is generic [21, 6], and therefore robust; hence, the statement of the theorem follows from Theorem 4.4. \square

Let us fix $\mu = 1/100$ in (42), so that the resulting CDS (43) becomes

$$\begin{aligned} \frac{dx_1}{dt} &= (80 - 100\beta) + \left(\frac{141}{5} + \beta\right) x_1 + \frac{6}{5}x_1^2 - \frac{179}{100}x_1x_2 - \frac{3}{250}x_1^2x_2 + \frac{3}{200}x_1x_2^2, \\ \frac{dx_2}{dt} &= 80 - \frac{409}{5}x_2 + \frac{1}{100}x_1x_2 + \frac{8}{5}x_2^2 - \frac{1}{125}x_2^3. \end{aligned} \quad (44)$$

It is found numerically that (44) undergoes the homoclinic bifurcation at $\beta \approx 50/5879$; state-space is displayed in Figure 5(d)–(e), and agrees well with that of the target DS (40).

CDS (44) is cubic. In Appendix F, we apply a generalized QCM to design a quadratic CDS undergoing super-critical homoclinic bifurcation.

5.4 Hilbert's 16th problem in chemistry

In 1900, David Hilbert presented a list of mathematical problems, 16th of which asks for the maximum number of limit cycles in two-dimensional n -degree polynomial DSs [22]. This number is denoted by $H(n)$, and remains unknown for all $n \geq 2$ [23]. One can pose a similar question in the chemical context: what is the maximum number of limit cycles in two-dimensional n -degree CDSs? We denote this number by $H_C(n)$. Let us show that chemical Hilbert number $H_C(n)$ is sandwiched between the two successive general Hilbert numbers $H(n-1)$ and $H(n)$.

Theorem 5.4. For every integer $n \geq 2$, if $H(n) < \infty$, then $H(n-1) \leq H_C(n) \leq H(n)$.

Proof. CDSs are a subset of polynomial DSs; hence, $H_C(n) \leq H(n)$. If $H(n) < \infty$, then $H(n-1) < \infty$ [24][Theorem 1]. Furthermore, then there exists a two-dimensional $(n-1)$ -degree DS with $H(n-1)$ hyperbolic limit cycles [24][Theorem 2(a)]. This DS can be mapped via a QCM to the two-dimensional n -degree CDS (26). It follows from Theorem 4.3(iii) that this CDSs has $H(n-1)$ limit cycles, implying that $H_C(n) \geq H(n-1)$. \square

Corollary 5.1. $H_C(3) \geq 4$, $H_C(4) \geq 13$, $H_C(5) \geq 28$, and $H_C(n) = \mathcal{O}(n^2 \ln(n))$ as $n \rightarrow \infty$.

Proof. Statement of the corollary follows from Theorem 5.4 and the fact that $H(2) \geq 4$ [25], $H(3) \geq 13$ [26], $H(4) \geq 28$ [27], and $H(n) = \mathcal{O}(n^2 \ln(n))$ as $n \rightarrow \infty$ [28]. \square

6 Discussion

In this paper, we have investigated *chemical maps* - special maps that transform general dynamical systems (DSs) into chemical dynamical systems (CDSs), while preserving desired features. We have introduced a novel chemical map, called the *quasi-chemical map* (QCM), which systematically perturbs any given polynomial DS in such a way that it becomes a CDS under sufficiently large translations. The QCM qualitatively preserves robust dynamical and bifurcation structures; see respectively Theorems 4.1 and 4.4. In particular, this map qualitatively preserves hyperbolic equilibria and limit cycles, temporal properties, such as periods of oscillations, as well as trapping regions; see Theorem 4.3. In addition, the QCM increases degree of DSs by at most one.

These properties can make the QCM more favorable than some alternative transformations, such as the time-change map [11, 12] and the \mathbf{x} -factorable map [14]. In particular, while the time-change map preserves trajectories in state-space, it does not preserve temporal properties; furthermore, it can significantly increase degree of DSs. On the other hand, while the \mathbf{x} -factorable map increases the degree by only one, it is not rigorously justified, and can fail to preserve even hyperbolic equilibria; see Section 3. In a special case, the QCM can be interpreted as a correction of the \mathbf{x} -factorable map; see Theorem 4.2.

In Section 5, we have applied the QCM to design some CDSs with exotic behaviors. In particular, in Section 5.1, we have designed CDS (30) with arbitrary many limit cycles. Another such CDS is designed in [29], with the goal of providing a lower bound on the maximum number of stable limit cycles in two-dimensional n -degree CDSs. This Hilbert-like number is denoted by $C(n)$, and the bound obtained in [29] is $C(n) \geq \lfloor (n+2)/6 \rfloor$, where $\lfloor \cdot \rfloor$ denotes the integer part of a real number. CDS (30) from Section 5.1 of this paper predicts a better bound, namely $C(n) \geq \lfloor (n+1)/4 \rfloor$.

In Section 5.2, we have designed a cubic CDS with Lorenz attractor. A similar system has been put forward in [14]; however, since the \mathbf{x} -factorable map is applied and some of the variables are translated differently, existence of the chaotic attractor is not rigorously justified. On the other hand, a CDS with Lorenz attractor rigorously justified is presented in [30]. To design it, the authors use the time-change map; consequently, the CDS is quartic and the time-scale at which the Lorenz attractor is tracked is distorted. In Section 5.3, we have presented a cubic CDS undergoing a supercritical homoclinic bifurcation. This problem has also been considered using the \mathbf{x} -factorable map and numerical simulations in [6]. Another CDS with the homoclinic bifurcation has been designed in Appendix F of this paper; notably, it is quadratic.

In this paper, we have focused on polynomial DSs. Assume now that we are given a *non-polynomial* DS with continuously differentiable vector field; assume also that this DS is robust in a desired state-space region. One approach to design a dynamically similar CDS is to first map the non-polynomial DS to a qualitatively equivalent polynomial DS; this can be done in a dimension-preserving manner using the Weierstrass approximation theorem, see Appendix G. Once a suitable

polynomial DS is found, one can then apply the QCM to obtain a qualitatively equivalent CDS. Another, more direct, approach to map robust non-polynomial DSs to CDSs is by using special chemical systems that execute suitable algorithms from the theory of artificial neural networks [31].

The chemical maps presented in this paper are *dimension-preserving*, i.e. they introduce no additional dependent variables. In a follow-up paper, we will focus on *dimension-expanding* chemical maps that introduce auxiliary variables to achieve chemical systems. As part of future research, we also formulate the following fundamental problem: *Find classes of polynomial DSs that can be mapped to CDSs with the same dimension and degree, and with desired dynamics preserved.* This general problem is also relevant to Hilbert’s 16th problem in chemistry. In particular, we have proved that $H_C(n) \geq H(n - 1)$ in Theorem 5.4 of Section 5.4, using the special QCM (26), which increases degree of DSs by one. A natural question is whether the more general QCM (24) can be applied to suitable polynomial DSs in a degree-preserving manner to probe if e.g. $H_C(n) = H(n)$ for some $n \geq 2$. As a step forward with the more general problem, we present the following result.

Theorem 6.1. *Consider the class of N -dimensional n -degree polynomial DSs*

$$\frac{dy_i}{dt} = f_i(\mathbf{y}) + \beta_i y_i^n, \quad i = 1, 2, \dots, N, \quad (45)$$

where $f_i \in \mathbb{P}_{n-1}(\mathbb{R}^N, \mathbb{R})$ are arbitrary polynomials of degree at most $(n - 1)$ for all $i = 1, 2, \dots, N$. Assume that for every $i = 1, 2, \dots, N$ such that $\beta_i \neq 0$ the following condition holds: $\beta_i < 0$ if $n \geq 1$ is odd, and $\beta_i > 0$ if $n \geq 2$ is even. Assume furthermore that (45) is robust in $\mathbb{U} \subset \mathbb{R}^N$. Then, N -dimensional n -degree CDS

$$\frac{dx_i}{dt} = \beta_i \left(x_i - \frac{T_i}{\mu} \right)^n + \frac{\mu}{T_i} x_i f_i \left(\mathbf{x} - \frac{\mathbf{T}}{\mu} \right), \quad i = 1, 2, \dots, N, \quad (46)$$

in $\mathbb{U} + \mathbf{T}/\mu \subset \mathbb{R}^N$ is qualitatively equivalent to DS (45) in \mathbb{U} .

Proof. Applying on (45) the QCM (24) with $q_i = \beta_i y_i^n$, one obtains (46). Statement of the theorem then follows from Theorem 4.1. \square

Let us remark that DSs of the form (45) can in two dimensions have arbitrary many limit cycles, and may display chaotic attractors in three dimensions; see Theorems 5.1 and E.1, which can be seen as special cases of Theorem 6.1.

A Background theory

In this section, we present further background theory.

Definition A.1. (Qualitative equivalence) Consider DS (2) in region $\mathbb{U} \subset \mathbb{R}^N$, and DS (4) in region $\mathbb{V} \subset \mathbb{R}^N$. Let Φ be a continuous map from \mathbb{U} onto \mathbb{V} , which has a continuous inverse. Assume that Φ maps solutions of (2) contained in \mathbb{U} onto the solutions of (4) contained in \mathbb{V} , and preserves the direction of time. Then, (2) in \mathbb{U} is said to be qualitatively equivalent to (4) in \mathbb{V} .

Definition A.2. (Robust solution) Let $\{\mathbf{y}(t; \mathbf{y}_0) | t \in [0, t_y]\}$ be a solution of (2) for some (possibly infinite) $t_y > 0$. Assume that for every neighborhood $\mathbb{U} \subset \mathbb{R}^N$ of $\{\mathbf{y}(t; \mathbf{y}_0) | t \in [0, t_y]\}$, and for every $\mathbf{F} \in C^1$ with $\mathbf{F}(\mathbf{z}; 0) = \mathbf{0}$, there exists $\mu_0 > 0$ such that for all $\mu \in (0, \mu_0)$ DS (3) has a solution $\{\mathbf{z}(t; \mathbf{y}_0) | t \in [0, t_z]\} \in \mathbb{U}$ such that (3) in a neighborhood of $\{\mathbf{z}(t; \mathbf{y}_0) | t \in [0, t_z]\}$ is qualitatively equivalent to (2) in a neighborhood of $\{\mathbf{y}(t; \mathbf{y}_0) | t \in [0, t_y]\}$. Then, solution $\mathbf{y}(t; \mathbf{y}_0)$ of (2) is robust.

Linearization. Let $\nabla\mathbf{f}(\mathbf{y}) \in \mathbb{R}^{N \times N}$ be the Jacobian matrix for (2), where $(\nabla\mathbf{f}(\mathbf{y}))_{i,j} = (\partial f_i(\mathbf{y})/\partial y_j)$. Then, the linearization around the solution $\mathbf{y}(t)$ of (2) is given by

$$\frac{d\mathbf{z}}{dt} = \nabla\mathbf{f}(\mathbf{y}(t))\mathbf{z}. \quad (47)$$

If \mathbf{y}^* is a time-independent solution of (2), then $\mathbf{z}(t) = \exp(\nabla\mathbf{f}(\mathbf{y}^*)t)\mathbf{z}_0$, and we associate the eigenvalues of $\nabla\mathbf{f}(\mathbf{y}^*)$ to \mathbf{y}^* .

Definition A.3. (*Equilibrium*) $\mathbf{y}^* \in \mathbb{R}^N$ is a hyperbolic equilibrium for (2) if:

- (i) $\mathbf{f}(\mathbf{y}^*) = \mathbf{0}$, and
- (ii) All N eigenvalues associated to \mathbf{y}^* have non-zero real parts.

Another important class of solutions of (2) are those that are periodic with period $\tau > 0$, which we denote by $\mathbf{y}_\tau = \mathbf{y}_\tau(t)$. In this case, the solution of the linearization (47) is of the form $\mathbf{z}(t) = P(t)\exp(At)\mathbf{z}_0$, where $P(t) \in \mathbb{R}^{N \times N}$ is a τ -periodic matrix, and $A \in \mathbb{R}^{N \times N}$ is time-independent [1]. We say that the eigenvalues of A are characteristic exponents associated to $\mathbf{y}_\tau(t)$; we note that at least one of the exponents has zero real part.

Definition A.4. (*Limit cycle*) $\mathbf{y}_\tau : \mathbb{R}_\geq \rightarrow \mathbb{R}^N$ is a hyperbolic limit cycle with period $\tau > 0$ for (2) if:

- (i) $\mathbf{y}_\tau(t)$ is a solution of (2) such that $\mathbf{y}_\tau(0) = \mathbf{y}_\tau(\tau)$ and $\mathbf{y}_\tau(0) \neq \mathbf{y}_\tau(t)$ for all $t \in (0, \tau)$, and
- (ii) $(N - 1)$ characteristic exponents associated to \mathbf{y}_τ have non-zero real parts.

Trapping regions. For solutions $\mathbf{y}(t)$ of (2) that are neither time-independent nor periodic, linearization (47) is more difficult to analyze. In this more general context, particularly important are regions of state-space on whose boundary vector field of a DS points inwards. Consequently, if the state of the DS is initiated inside such a region, then it stays in there for all future times.

Definition A.5. (*Trapping region*) Let $\mathbb{S} = \{\mathbf{y} \in \mathbb{R}^N | V(\mathbf{y}) \leq r \text{ for some } r > 0\}$ be a compact set in state-space, where $V : \mathbb{R}^N \rightarrow \mathbb{R}$ is a continuous function such that the boundary $V(\mathbf{y}) = r$ has a well-defined normal at each point. If vector field $\mathbf{f}(\mathbf{y})$ points inwards on the boundary $V(\mathbf{y}) = r$, then \mathbb{S} is called a trapping region for (2).

Remark. A sufficient condition for $V(\mathbf{y}) = r$ to have a well-defined normal at each point is that $V : \mathbb{R}^N \rightarrow \mathbb{R}$ is continuously differentiable and that $\nabla V(\mathbf{y}) \neq \mathbf{0}$ for all $\mathbf{y} \in \mathbb{R}^N$ such that $V(\mathbf{y}) = r$.

A.1 Chemical reaction networks

Every CDS induces a canonical set of chemical reactions [3]. To state this result, given any $x \in \mathbb{R}$, we define the sign function as $\text{sign}(x) = -1$ if $x < 0$, $\text{sign}(x) = 0$ if $x = 0$, and $\text{sign}(x) = 1$ if $x > 0$.

Definition A.6. (*Chemical reaction network*) Assume that (4) is a CDS, i.e. $\mathbf{g} \in \mathbb{P}_n^C(\mathbb{R}^N, \mathbb{R}^N)$. Let $\alpha x_1^{\nu_1} x_2^{\nu_2} \dots x_N^{\nu_N}$, with $\alpha \in \mathbb{R}$ and $\nu_1, \nu_2, \dots, \nu_N \in \mathbb{Z}_\geq$, be a monomial from g_i . Then, monomial $\alpha x_1^{\nu_1} x_2^{\nu_2} \dots x_N^{\nu_N} = \text{sign}(\alpha)|\alpha|x_1^{\nu_1} x_2^{\nu_2} \dots x_N^{\nu_N}$ induces the canonical chemical reaction

$$\sum_{k=1}^N \nu_k X_k \xrightarrow{|\alpha|} (\nu_i + \text{sign}(\alpha)) X_i + \sum_{k=1, k \neq i}^N \nu_k X_k, \quad (48)$$

where X_i denotes the chemical species whose concentration is x_i . The set of all such chemical reactions, induced by all the distinct monomials in \mathbf{g} , is called the canonical chemical reaction network (CRN) induced by (4).

Remark. Species on the left-hand side of (48) are called the *reactants*, while $|\alpha|$ is called the *rate coefficient*. Terms of the form $0X_i$ are denoted by \emptyset , and interpreted as some neglected species.

For any given CDS, the induced canonical CRN from Definition A.6 is unique. However, a given CDS can also induce other, non-canonical, CRNs.

Definition A.7. (Fused reaction) Consider M canonical reactions that have identical reactants and rate coefficients:

$$\sum_{k=1}^N \nu_k X_k \xrightarrow{|\alpha|} (\nu_{k_j} + \text{sign}(\alpha)) X_{k_j} + \sum_{k=1, k \neq k_j}^N \nu_k X_k, \quad j = 1, 2, \dots, M.$$

Then, the corresponding fused reaction is given by

$$\sum_{k=1}^N \nu_k X_k \xrightarrow{|\alpha|} (\nu_{k_1} + \text{sign}(\alpha)) X_{k_1} + \dots + (\nu_{k_M} + \text{sign}(\alpha)) X_{k_M} + \sum_{\substack{k=1, \\ k \neq k_1, k_2, \dots, k_M}}^N \nu_k X_k.$$

Any network obtained by fusing reactions in the canonical CRN is called a *non-canonical CRN*.

Example. The canonical CRN induced by (7) is given by (8). Since reactions $X_1 \xrightarrow{2} 2X_1$ and $X_1 \xrightarrow{2} X_1 + X_2$ from (8) have the same reactants and rate coefficients, they can be fused; the resulting non-canonical CRN is given (9).

B Appendix: Time-change map

Definition B.1. (Time-change map) Consider DS (1). Assume that $f_i \in \mathbb{P}_n^N(\mathbb{R}^N; \mathbb{R})$ for $i = 1, 2, \dots, K$, and $f_i \in \mathbb{P}_n^C(\mathbb{R}^N; \mathbb{R})$ for $i = K + 1, K + 2, \dots, N$. Consider CDS

$$\frac{dx_i}{ds} = (x_1 x_2 \dots x_K) f_i(\mathbf{x}), \quad i = 1, 2, \dots, N. \quad (49)$$

$\Psi_s : \mathbb{P}_n^N(\mathbb{R}^N; \mathbb{R}^N) \rightarrow \mathbb{P}_{n+K}^C(\mathbb{R}^N; \mathbb{R}^N)$, mapping the vector field of DS (1) to the vector field of CDS (49), is called a *time-change map*.

The time-change map can be interpreted as a state-dependent time-rescaling in (1).

Theorem B.1. Consider DS (1) with $f_i \in \mathbb{P}_n^N(\mathbb{R}^N; \mathbb{R})$ for $i = 1, 2, \dots, K$, and $f_i \in \mathbb{P}_n^C(\mathbb{R}^N; \mathbb{R})$ for $i = K + 1, K + 2, \dots, N$. Assume that (1) with initial condition $\mathbf{y}_0 = (y_{1,0}, \dots, y_{N,0})^\top \in \mathbb{R}_{>}^N$ with $(y_{1,0}, \dots, y_{K,0})^\top \in \mathbb{R}_{>}^K$ has a solution $\mathbf{y}(t; \mathbf{y}_0) \in \mathbb{R}_{\geq}^N$ with $(y_1(t; \mathbf{y}_0), \dots, y_K(t; \mathbf{y}_0))^\top \in \mathbb{R}_{>}^K$ for all $t \in [0, t_0]$ for some $t_0 > 0$. Then, CDS (49) has the solution $\mathbf{y}(t(s); \mathbf{y}_0) \in \mathbb{R}_{\geq}^N$ for all $s \in [0, \int_0^{t_0} (y_1(\theta; \mathbf{y}_0) \dots y_K(\theta; \mathbf{y}_0))^{-1} d\theta]$, where $t(s)$ is the inverse of $s(t) = \int_0^t (y_1(\theta; \mathbf{y}_0) \dots y_K(\theta; \mathbf{y}_0))^{-1} d\theta$.

Proof. Since $(y_1(t; \mathbf{y}_0), \dots, y_K(t; \mathbf{y}_0))^\top \in \mathbb{R}_{>}^K$ for all $t \in [0, t_0]$, it follows that $s(t)$ is then well-defined and $s(t) > 0$; furthermore, $s(t)$ is monotonically increasing for all $t \in [0, t_0]$ and, hence, has an inverse then, which we denote by $t(s)$. Let $x_i(s; \mathbf{y}_0) = y_i(t(s); \mathbf{y}_0)$; then, it follows from (1) that for all $s \in [0, \int_0^{t_0} (y_1(\theta; \mathbf{y}_0) \dots y_K(\theta; \mathbf{y}_0))^{-1} d\theta]$ variable $x_i = x_i(s; \mathbf{y}_0)$ satisfies

$$\frac{dx_i}{ds} = \frac{dy_i}{dt} \frac{dt}{ds} = (x_1 \dots x_K) f_i(\mathbf{x}), \quad i = 1, 2, \dots, N, \quad (50)$$

which is identical to (49). □

Remark. More generally, monomial $(x_1 x_2 \dots x_K)$ from (49) can be replaced with any other polynomial that ensures (49) is chemical; for example, $(x_1^{n_1} x_2^{n_2} \dots x_K^{n_K})$ with $n_i \in \mathbb{Z}_>$ is allowed.

Remark. Assume that a solution of (1) is bounded for all $t \geq 0$; then, such a solution can be translated to the positive orthant prior to applying the time-change map. Therefore, Theorem B.1 shows that such translated time-change map can preserve any bounded solution, such as equilibria and limit cycles.

C Appendix: Generalized quasi-chemical map

In this section, we present a more general form of the QCM. To this end, we define vector $\mathbf{T}_{\mu, \mathbf{a}} = (T_1/\mu^{a_1}, \dots, T_N/\mu^{a_N})^\top \in \mathbb{R}_{\geq}^N$ and diagonal matrix $S_{\mu, \mathbf{b}} = \text{diag}(s_1/\mu^{b_1}, \dots, s_N/\mu^{b_N}) \in \mathbb{R}_{>}^{N \times N}$, where $T_i \geq 0$, $s_i > 0$, and $a_i, b_i \in \mathbb{Z}_{\geq}$ are fixed parameters, while $\mu > 0$ is a free parameter. Furthermore, we let $p_i(\cdot; \mu) \in \mathbb{P}_n(\mathbb{R}^N, \mathbb{R})$ be polynomials that are continuously differentiable in μ with $p_i(\mathbf{z}; 0) = 0$.

Definition C.1. (*Generalized quasi-chemical map*) Consider DS (1). Consider also

$$\begin{aligned} \frac{\mu^{b_i}}{s_i} \frac{dx_i}{dt} &= \left[q_i \left(S_{\mu, \mathbf{b}}^{-1}(\mathbf{x} - \mathbf{T}_{\mu, \mathbf{a}}) \right) + p_i \left(S_{\mu, \mathbf{b}}^{-1}(\mathbf{x} - \mathbf{T}_{\mu, \mathbf{a}}); \mu \right) \right] \\ &\quad + \frac{\mu^{a_i}}{T_i} x_i \left[f_i \left(S_{\mu, \mathbf{b}}^{-1}(\mathbf{x} - \mathbf{T}_{\mu, \mathbf{a}}) \right) - q_i \left(S_{\mu, \mathbf{b}}^{-1}(\mathbf{x} - \mathbf{T}_{\mu, \mathbf{a}}) \right) \right], \quad i = 1, 2, \dots, N. \end{aligned} \quad (51)$$

Assume that $[q_i(S_{\mu, \mathbf{b}}^{-1}(\mathbf{x} - \mathbf{T}_{\mu, \mathbf{a}})) + p_i(S_{\mu, \mathbf{b}}^{-1}(\mathbf{x} - \mathbf{T}_{\mu, \mathbf{a}}); \mu)] \in \mathbb{P}_n^{\mathcal{C}}(\mathbb{R}^N, \mathbb{R})$ is chemical for all sufficiently small $\mu > 0$ and for all $i = 1, 2, \dots, N$. Assume also that $a_i > b_i$ for all $i = 1, 2, \dots, N$. Then, $\Psi_\mu : \mathbb{P}_n(\mathbb{R}^N, \mathbb{R}^N) \rightarrow \mathbb{P}_{n+1}^{\mathcal{C}}(\mathbb{R}^N, \mathbb{R}^N)$, mapping the vector field of DS (1) to the vector field of CDS (51) for all sufficiently small $\mu > 0$, is called a quasi-chemical map.

Remark. Definition C.1 can be further generalized by replacing the diagonal matrix $S_{\mu, \mathbf{b}} \in \mathbb{R}^{N \times N}$ with general matrix $A_\mu \in \mathbb{R}^{N \times N}$ that is non-singular for all sufficiently small $\mu > 0$.

Lemma C.1. Under the affine change of variables $z_i = (\mu^{b_i}/s_i)(x_i - T_i/\mu^{a_i})$ for every $\mu > 0$, DS (51) becomes

$$\frac{dz_i}{dt} = f_i(\mathbf{z}) + p_i(\mathbf{z}; \mu) + \mu^{a_i - b_i} \frac{s_i}{T_i} z_i [f_i(\mathbf{z}) - q_i(\mathbf{z})], \quad i = 1, 2, \dots, N. \quad (52)$$

Comparing Lemma C.1 with Lemma 4.1, one can notice that, in addition to translation, the generalized QCM also involves scaling of the dependent variables, as well as additional perturbations $p_i(\mathbf{z}; \mu)$; furthermore, different variables can be scaled differently. It follows from Lemma C.1, and the assumption $a_i > b_i$, that the generalized QCM obeys analogous results as those presented in Section 4. For example, Theorem 4.3 holds, but with a different error estimates, namely $\mathcal{O}(\mu^\kappa)$, where $\kappa > 0$ is the minimum value in $\{a_1 - b_1, a_2 - b_2, \dots, a_N - b_N\}$.

Special case. To obtain an analogue of (26), we choose $q_i = p_i = 0$ in (51), leading to

$$\frac{dx_i}{dt} = \mu^{a_i - b_i} \frac{s_i}{T_i} x_i f_i \left(S_\mu^{-1}(\mathbf{x} - \mathbf{T}_{\mu, \mathbf{a}}) \right), \quad i = 1, 2, \dots, N. \quad (53)$$

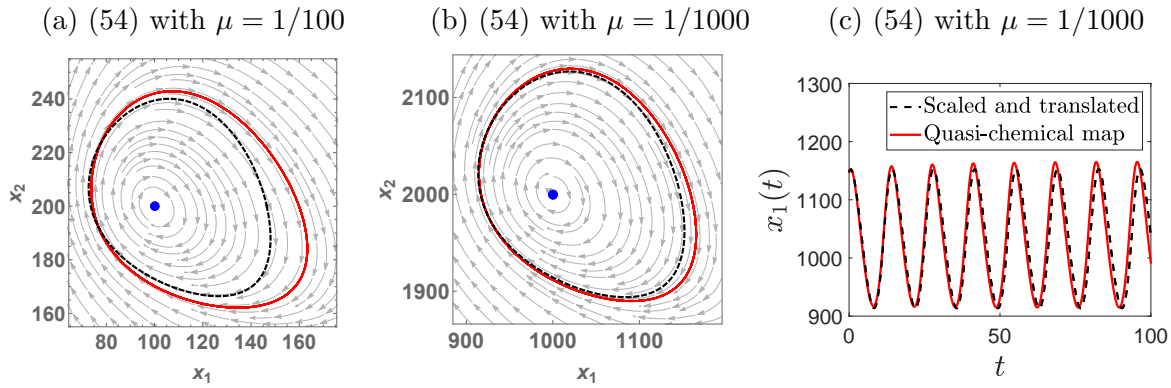


Figure 6: Application of the generalized QCM (51) on DS (16). Panel (a) displays state-space for (54) with $\mu = 1/100$, with the limit cycle shown as the solid red curve, and the equilibrium as the blue dot; also shown as dashed black curve is the limit cycle of (16) under the same scaling and translation as in (54). Panel (b) displays the same plot for $\mu = 1/1000$, while panel (c) displays a corresponding time-state space.

Example. Let us apply on (16) the QCM (51) with $q_1 = 0$, $q_2 = f_2$, $p_1 = p_2 = 0$, $T_1 = 1$, $T_2 = 2$, $a_1 = a_2 = 1$, $s_1 = s_2 = 1$ and $b_1 = b_2 = 1/2$, which leads to

$$\begin{aligned} \frac{dx_1}{dt} &= \mu x_1 \left[\frac{1}{2} \left(x_2 - \frac{2}{\mu} \right) + \frac{1}{8} \left(x_1 - \frac{1}{\mu} \right) \right], \\ \frac{dx_2}{dt} &= -\frac{1}{2} \left(x_1 - \frac{1}{\mu} \right) - \mu^{1/2} \frac{1}{20} \left(x_1 - \frac{1}{\mu} \right) \left(x_2 - \frac{2}{\mu} \right) + \mu^{1/2} \frac{1}{20} \left(x_2 - \frac{2}{\mu} \right)^2 - \frac{3}{32} \left(x_2 - \frac{2}{\mu} \right). \end{aligned} \quad (54)$$

One can readily show that (54) is chemical for all sufficiently small $\mu > 0$. In Figure 6(a), we display state-space for (54) when $\mu = 1/100$. Analogous plot is shown in Figure 6(b) for $\mu = 1/1000$, with a corresponding time-state space shown in Figure 6(c). These plots confirm that the limit cycle is now of order $\mathcal{O}(\mu^{-1/2})$, as opposed to $\mathcal{O}(1)$ as in Figure 2. Note that the error between the limit cycle of (54) and that of suitably scaled and translated target system, as well as their periods, is $\mathcal{O}(\mu^{1/2})$, as opposed to $\mathcal{O}(\mu)$ as in Figure 2; in particular, the convergence order is now lower due to the magnification of the limit cycle.

D Appendix: Perturbed harmonic oscillator

Lemma D.1. Consider the perturbed harmonic oscillator given by (29). Let $0 < r_1 < r_2 < \dots < r_n$ be arbitrary real numbers. Then, there exists coefficients $\beta_i = \beta_i(r_1, r_2, \dots, r_n)$ for $i = 0, 1, \dots, N$ such that for every sufficiently small $\varepsilon > 0$ system (29) has n nested limit cycles. The i th limit cycle is arbitrarily close to $y_1(t) = r_i \cos(t)$ and $y_2(t) = -r_i \sin(t)$, and has period arbitrarily close to 2π . The n th limit cycle is stable, and the limit cycles alternate in stability.

Proof. Substituting $f_1 = \beta_0 y_1 + \beta_1 y_1^3 + \beta_2 y_1^5 + \dots + \beta_n y_1^{2n+1}$ and $f_2 = 0$ into

$$I(r) = \int_0^{2\pi} \left[f_1(r \cos(s), -r \sin(s)) \cos(s) - f_2(r \cos(s), -r \sin(s)) \sin(s) \right] ds,$$

one obtains

$$I(r) = \pi r \sum_{i=0}^n 2^{-2i} \binom{2i+1}{i+1} \beta_i r^{2i}, \quad (55)$$

where we use $\int_0^{2\pi} \cos^{2n}(t) dt = 2^{-2n+2} \binom{2n-1}{n} \pi$. Using Vieta's formulas, it follows that $0 < r_1^2 <$

$r_2^2 < \dots < r_n^2$ are the roots of $I(r)$ if

$$\beta_i = (-1)^{n-i+1} 2^{2i} \binom{2i+1}{i+1}^{-1} \sum_{l \in C_{n-i}^n} (r_{l(1)} r_{l(2)} \dots r_{l(n-i)})^2 \quad \text{for all } i = 0, 1, 2, \dots, n-1,$$

$$\beta_n = -2^{2n} \binom{2n+1}{n+1}^{-1}, \quad (56)$$

where C_k^n denotes the set of all combinations of length $1 \leq k \leq n$ of the elements from $\{1, 2, \dots, n\}$. Simple zeros of $I(r)$ correspond to the hyperbolic limit cycles of (29), and their stability is determined by the slope of $I(r)$ [1][Chapter 4.9], implying the statement of the lemma. \square

Remark. We impose that $2^{-2n} \binom{2n+1}{n+1} \beta_n < 0$ to ensure stability of the limit cycle with radius r_n ; we arbitrarily let $2^{-2n} \binom{2n+1}{n+1} \beta_n = -1$.

Rate coefficients for (30). The coefficients are given by

$$\alpha_i = \left| \delta_0(i) \frac{1}{\mu} + \varepsilon \sum_{j=0}^n \beta_j \binom{2j+1}{i} \left(\frac{1}{\mu} \right)^{2j+1-i} \right|, \quad i = 0, 1, \dots, 2n+1, \quad \alpha_{2n+2} = 1, \quad \alpha_{2n+3} = \mu, \quad (57)$$

where $\beta_0, \beta_1, \dots, \beta_n$ are given by (56), and $\delta_i(j)$ be the Kronecker-delta, i.e. $\delta_i(j) = 1$ if $j = i$, and $\delta_i(j) = 0$ otherwise.

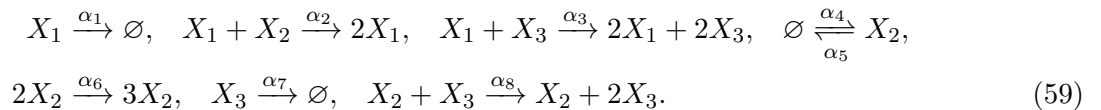
E Appendix: Candidate quadratic CRN with chaos

Chemical Lorenz system (39) contains a cubic term, i.e. CRN (36) contains one tri-molecular reaction. Let us now focus on deriving a quadratic CDS with chaos. To this end, consider the DS

$$\begin{aligned} \frac{dy_1}{dt} &= \frac{27}{10} y_2 + y_3, \\ \frac{dy_2}{dt} &= -y_1 + y_2^2, \\ \frac{dy_3}{dt} &= y_1 + y_2, \end{aligned} \quad (58)$$

which has been put forward as displaying a chaotic attractor in [32] as ‘‘Case P’’. This attractor has been numerically investigated, see also Figure 7(a)–(b); however, no rigorous proofs are given. Note that proving existence and properties of chaotic attractors can be a difficult task. For example, there is a gap of more than three decades between numerical evidence of the Lorenz attractor [19] and its rigorous proof [20]. To proceed, in this paper we simply assume that (58) has a robust chaotic attractor, which allows us to state the following result.

Theorem E.1. (Quadratic CRN with a chaotic attractor) *Assume that DS (58) has a chaotic attractor which is robust. Consider the CRN*



Assume that the rate coefficients are given by

$$\alpha_1 = 2, \quad \alpha_2 = \frac{27}{10}\mu, \quad \alpha_3 = \mu, \quad \alpha_4 = \frac{100}{729\mu^2}, \quad \alpha_5 = \frac{20}{27\mu} - \frac{27}{10}, \quad \alpha_6 = 1, \quad \alpha_7 = \frac{37}{27}, \quad \alpha_8 = \mu. \quad (60)$$

Then, for every sufficiently small $\mu > 0$, CRN (59) has a chaotic attractor which is qualitatively equivalent to the robust chaotic attractor of (58).

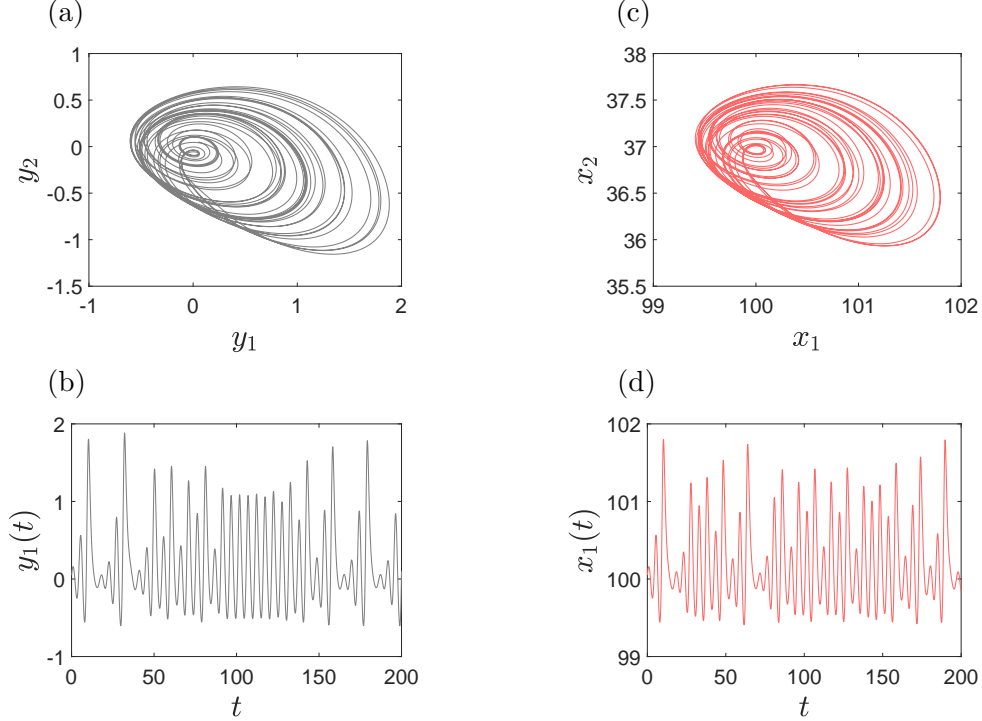


Figure 7: Quadratic CDS with chaos. Panels (a)–(b) display (y_1, y_2) - and (t, y_1) -space for DS (58), with initial condition $y_1(0) = y_2(0) = y_3(0) = 5/100$. Panels (c)–(d) show analogous plots for CDS (62) with initial condition $x_1(0) = x_3(0) = 5/100 + 100$ and $x_2(0) = 5/100 + 1000/27$.

Proof. Let us apply on DS (58) the QCM (24) with $T_1 = T_3 = 1$, $T_2 = 10/27$, $q_1 = q_3 = 0$ and $q_2 = y_2^2$, leading to the CDS

$$\begin{aligned} \frac{dx_1}{dt} &= \mu x_1 \left[\frac{27}{10} \left(x_2 - \frac{10}{27\mu} \right) + \left(x_3 - \frac{1}{\mu} \right) \right], \\ \frac{dx_2}{dt} &= \left(x_2 - \frac{10}{27\mu} \right)^2 + \frac{27}{10} \mu x_2 \left[- \left(x_1 - \frac{1}{\mu} \right) \right], \\ \frac{dx_3}{dt} &= \mu x_3 \left[\left(x_1 - \frac{1}{\mu} \right) + \left(x_2 - \frac{10}{27\mu} \right) \right]. \end{aligned} \quad (61)$$

An induced CRN is given by (59), with rate coefficients (60). Using the assumption that (58) has a robust attractor, the statement of the theorem follows from Theorem 4.1. \square

Remark. The choice of the translation parameters has been made so that the monomial x_1x_2 appears with the same coefficient in the first two equations in (61), allowing for fusing of the underlying canonical reactions; see Definition A.7.

Remark. The assumption in Theorem E.1 can be weakened: it is sufficient to assume that (58) has a chaotic attractor which is robust with respect to only the chemical perturbations underlying (61); see also the remark below Theorem 4.1.

Let us fix $\mu = 1/100$ in (60), under which CDS (61) becomes

$$\begin{aligned}\frac{dx_1}{dt} &= -2x_1 + \frac{27}{1000}x_1x_2 + \frac{1}{100}x_1x_3, \\ \frac{dx_2}{dt} &= \frac{10^6}{729} - \frac{19271}{270}x_2 - \frac{27}{1000}x_1x_2 + x_2^2, \\ \frac{dx_3}{dt} &= -\frac{37}{27}x_3 + \frac{1}{100}x_1x_3 + \frac{1}{100}x_2x_3.\end{aligned}\tag{62}$$

Dynamics of (62) is shown in Figure 7(c)–(d), which compares well with the original DS (58).

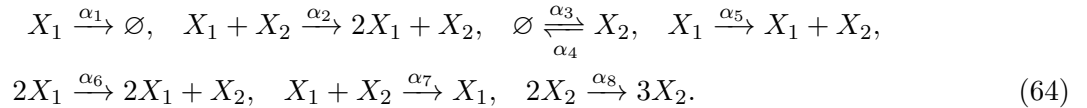
F Appendix: Quadratic CRN with homoclinic bifurcation

Consider the DS

$$\begin{aligned}\frac{dy_1}{dt} &= y_2, \\ \frac{dy_2}{dt} &= y_1 + \beta y_2 + y_1^2 - y_1y_2,\end{aligned}\tag{63}$$

which undergoes a super-critical homoclinic bifurcation [1][Chapter 4.8].

Theorem F.1. (*Quadratic CRN with homoclinic bifurcation*) Consider the CRN



Assume that the rate coefficients are given by

$$\begin{aligned}\alpha_1 = \frac{1}{\mu^{1/2}}, \quad \alpha_2 = \mu^{1/2}, \quad \alpha_3 = \frac{1}{\mu^{5/3}} - \frac{1}{\mu^{3/2}} + \frac{1}{\mu} - \frac{1}{\mu^{1/2}}, \quad \alpha_4 = \frac{2}{\mu^{2/3}} - \frac{1}{\mu^{1/2}}, \\ \alpha_5 = \frac{1}{\mu} - \frac{2 + \beta}{\mu} + 1, \quad \alpha_6 = 1, \quad \alpha_7 = 1 - \beta\mu^{1/2}, \quad \alpha_8 = \mu^{1/3}.\end{aligned}\tag{65}$$

Then, for every sufficiently small $\mu > 0$, CRN (64) undergoes a super-critical homoclinic bifurcation at saddle $(1/\mu^{1/2}, 1/\mu) \in \mathbb{R}_>^2$ at some parameter value $\beta = \beta(\mu) \in (-1, 0)$.

Proof. Consider the perturbed DS

$$\begin{aligned}\frac{dz_1}{dt} &= f_1(z_1, z_2) = z_2 + \mu^{1/2}z_1z_2, \\ \frac{dz_2}{dt} &= f_2(z_1, z_2; \beta) = z_1 + \beta \left(z_2 + \mu^{1/2}z_1z_2 \right) + z_1^2 - z_1z_2 + \mu^{1/3}z_2^2.\end{aligned}\tag{66}$$

The angle between the vector field of (66) and the z_1 -axis is given by $\theta = \tan^{-1}[f_2(z_1, z_2)/f_1(z_1, z_2; \beta)]$, and hence satisfies the differential equation

$$\frac{d\theta}{d\beta} = \frac{f_1(z_1, z_2) \frac{\partial f_2(z_1, z_2; \beta)}{\partial \beta}}{f_1^2(z_1, z_2) + f_2^2(z_1, z_2; \beta)} = \frac{f_1^2(z_1, z_2)}{f_1^2(z_1, z_2) + f_2^2(z_1, z_2; \beta)}. \quad (67)$$

Hence, for points in the state-space which are not equilibria, the vector field rotates anti-clockwise as parameter β is increased. If $\mu = 0$, then (66) has a stable hyperbolic limit cycle with clockwise orientation for a range of values $\beta > -1$ [1][Chapter 4.8]; hence, the same is true for (66) for all sufficiently small $\mu > 0$. It follows from (67) and [1][Chapter 4.6] that this limit cycle monotonically expands as β is increased, until it forms a stable homoclinic loop at the saddle $(0, 0)$ at some bifurcation value $\beta(\mu) > -1$. Since the homoclinic loop is stable, it follows that the trace of Jacobian for (66) at $(0, 0)$ is negative at the bifurcation, i.e. $\beta(\mu) < 0$ [1][Chapter 4.8]. Choosing a sufficiently small $\mu > 0$, restricting $\beta \in (-1, 0)$, and applying translation $x_1 = (z_1 + 1/\mu^{1/2})$ and $x_2 = (z_2 + 1/\mu)$, DS (66) becomes the CDS

$$\begin{aligned} \frac{dx_1}{dt} &= \mu^{1/2} x_1 \left(x_2 - \frac{1}{\mu} \right), \\ \frac{dx_2}{dt} &= \left(x_1 - \frac{1}{\mu^{1/2}} \right) + \beta \left[\left(x_2 - \frac{1}{\mu} \right) + \mu^{1/2} \left(x_1 - \frac{1}{\mu^{1/2}} \right) \left(x_2 - \frac{1}{\mu} \right) \right] + \left(x_1 - \frac{1}{\mu^{1/2}} \right)^2 \\ &\quad - \left(x_1 - \frac{1}{\mu^{1/2}} \right) \left(x_2 - \frac{1}{\mu} \right) + \mu^{1/3} \left(x_2 - \frac{1}{\mu} \right)^2, \end{aligned} \quad (68)$$

with a CRN given by (64)–(65). □

Remark. CDS (68) can also be obtained by applying on (63) the QCM (51) with $q_1 = 0$, $p_1 = 0$, $T_1 = 1$, $a_1 = 1/2$, $s_1 = 1$, $b_1 = 0$, $q_2 = f_2$, $p_2 = \mu^{1/2} \beta y_1 y_2 + \mu^{1/3} y_2^2$, $T_2 = 1$, $a_2 = 1$, $s_2 = 1$, $b_2 = 0$. One can introduce parameter $\varepsilon \equiv \mu^{1/6}$ to obtain continuously differentiable perturbations in (66).

Fixing $\mu = 1/100$ in (68), one obtains the CDS

$$\begin{aligned} \frac{dx_1}{dt} &= -10x_1 + \frac{1}{10}x_1x_2, \\ \frac{dx_2}{dt} &= \left(-910 + 10^{10/3} \right) + (81 - 10\beta)x_1 + (10 - 2 \times 10^{4/3})x_2 + x_1^2 + \left(-1 + \frac{\beta}{10} \right) x_1x_2 + \frac{1}{10^{2/3}}x_2^2, \end{aligned} \quad (69)$$

which is found numerically to undergo the homoclinic bifurcation at saddle $(10, 100)$ when $\beta \approx \frac{-191}{200}$.

G Appendix: Non-polynomial dynamical systems

Let us consider DSs with continuously differentiable vector fields,

$$\frac{dy}{dt} = \mathbf{h}(\mathbf{y}), \quad \text{where } \mathbf{h} \in C^1(\mathbb{R}^N, \mathbb{R}^N). \quad (70)$$

Theorem G.1. *Assume that vector field $\mathbf{h} \in C^1(\mathbb{R}^N, \mathbb{R}^N)$ is non-polynomial. Assume furthermore that (70) is robust in $\mathbb{U} \subset \mathbb{R}^N$. Then, there exists an N -dimensional polynomial DS (2) that is in \mathbb{U} qualitatively equivalent to N -dimensional non-polynomial DS (70) in \mathbb{U} .*

Proof. The Weierstrass approximation theorem [33][Theorem 1.6.2] guarantees that for every $\varepsilon > 0$ there exists a polynomial function $\mathbf{f}_\varepsilon : \mathbb{U} \rightarrow \mathbb{R}^N$ and a continuously differentiable function $\mathbf{F}_\varepsilon \in C^1(\mathbb{R}^N, \mathbb{R}^N)$ such that $\mathbf{h}(\mathbf{y}) = \mathbf{f}_\varepsilon(\mathbf{y}) + \mathbf{F}_\varepsilon(\mathbf{y})$ for all $\mathbf{y} \in \mathbb{U}$, where $\max_{\mathbf{y} \in \mathbb{U}}(\|\mathbf{F}_\varepsilon(\mathbf{y})\| + \|\nabla \mathbf{F}_\varepsilon(\mathbf{y})\|) < \varepsilon$. Using the assumption that (70) is robust in \mathbb{U} , it follows that for every sufficiently small $\varepsilon > 0$ DS (2) with vector field $\mathbf{f}_\varepsilon(\mathbf{y}) = \mathbf{h}(\mathbf{y}) - \mathbf{F}_\varepsilon(\mathbf{y})$ is qualitatively equivalent to DS (70) in \mathbb{U} , implying the statement of the theorem. \square

References

- [1] Perko, L., 2001. *Differential Equations and Dynamical Systems*. 3rd Edition, Springer-Verlag.
- [2] Feinberg, M. *Lectures on chemical reaction networks*. Delivered at the Mathematics Research Center, University of Wisconsin, 1979.
- [3] Érdi, P., Tóth, J. *Mathematical models of chemical reactions. Theory and applications of deterministic and stochastic Models*. Manchester University Press, Princeton University Press, 1989.
- [4] Endy D., 2005. Foundations for engineering biology. *Nature*, **484**: 449–453.
- [5] Soloveichik, D., Seeing G., Winfree E., 2010. DNA as a universal substrate for chemical kinetics. *Proceedings of the National Academy of Sciences*, **107**(12): 5393–5398.
- [6] Plesa, T., Vejchodský, T., and Erban, R., 2016. Chemical reaction systems with a homoclinic bifurcation: An inverse problem. *Journal of Mathematical Chemistry*, **54**(10): 1884–1915.
- [7] Plesa, T., Vejchodský, T., and Erban, R., 2017. Test models for statistical inference: Two-dimensional reaction systems displaying limit cycle bifurcations and bistability, 2017. *Stochastic Dynamical Systems, Multiscale Modeling, Asymptotics and Numerical Methods for Computational Cellular Biology*.
- [8] Plesa, T., and Zygalakis, K. C., Anderson, D. F., and Erban, R., 2018. Noise control for molecular computing. *Journal of the Royal Society Interface*, **15**(144): 20180199.
- [9] T. Plesa, G. B. Stan, T. E. Ouldridge, and W. Bae., 2021. Quasi-robust control of biochemical reaction networks via stochastic morphing. *Journal of the Royal Society Interface*, **18**: 1820200985.
- [10] Plesa, T., Dack, A., and Ouldridge, T. E., 2023. Integral feedback in synthetic biology: Negative-equilibrium catastrophe. *Journal of Mathematical Chemistry*, **61**: 1980–2018.
- [11] Figueiredo, A., Gleria, I.M., Rocha, T.M., 2000. Boundedness of solutions and Lyapunov functions in quasi-polynomial systems. *Phys. Lett. A*, **268**: 335–341.
- [12] Hangos, K.M., Szederkényi, G., 2011. Mass action realizations of reaction kinetic system models on various time scales. *J. Phys.: Conf. Ser.*, **268**: 012009.
- [13] Plesa, T., 2023. Stochastic approximations of higher-molecular by bi-molecular reactions. *Journal of Mathematical Biology*, **86**(2): 28.
- [14] Samardzija, N., Greller, L.D., Wasserman, E., 1989. Nonlinear chemical kinetic schemes derived from mechanical and electrical dynamical systems. *J. Chem. Phys.* **90**: 2296–2304.

- [15] Kuznetsov, Y. A., 1998. Elements of applied bifurcation theory. Springer, Berlin.
- [16] Escher, C., 1981. Bifurcation and coexistence of several limit cycles in models of open two-variable quadratic mass-action systems. *Chem. Phys.*, **63(3)**:337–348.
- [17] Coddington, A. and Levinson, N. *Theory of Ordinary Differential Equations*. McGraw-Hill, New-York, 1955.
- [18] Eckweiler, H. J., 1946. Nonlinear differential equations of the van der Pol type with a variety of periodic solutions. *Studies in Nonlinear Vibration Theory*, Institute of Mathematics and Mechanics, New York University.
- [19] Lorenz, E. N., 1963. Deterministic nonperiodic flow. *Journal of Atmospheric Sciences*, **20(2)**: 130–141.
- [20] Tucker, W., 1999. The Lorenz attractor exists. *Comptes Rendus de l'Académie des Sciences-Series I-Mathematics*, **328(12)**: 1197–1202.
- [21] Sandstede, B., 1997. Constructing dynamical systems having homoclinic bifurcation points of codimension two. *Journal of Dynamics and Differential Equations*, Vol. 9, No. 2., **4**: 296–288.
- [22] Hilbert, D., 1902. Mathematical problems. *Bulletin of the American Mathematical Society*, **80**: 437–479.
- [23] Ilyashenko, Y., 2002. Centennial history of Hilbert’s 16th problem. *Bulletin of the American Mathematical Society*, **39(3)**: 301–354.
- [24] Gasull, A., Santana, P., 2024. A note on Hilbert 16th Problem. Available as: <https://arxiv.org/abs/2407.13465>.
- [25] Chen, L., Wang, M., 1979. The relative position, and the number, of limit cycles of a quadratic differential system. *Acta Math. Sinica (Chin. Ser.)* **22**: 751–758.
- [26] Li, C., Liu, C., Yang, J., 2009. A cubic system with thirteen limit cycles. *J. Differ. Equations* **246(9)**: 3609–3619.
- [27] Prohens, R., Torregrosa, J., 2019. New lower bounds for the Hilbert numbers using reversible centers. *Nonlinearity* **32(1)**: 331–355.
- [28] Christopher, C.J., and Lloyd, N.G., 1995. Polynomial Systems: A Lower Bound for the Hilbert Numbers. *Proceedings: Mathematical and Physical Sciences*, **450**: 219–224.
- [29] Erban, R., Kang, H.W., 2023. Chemical Systems with Limit Cycles. *Bull Math Biol* **85**, 76.
- [30] Susits, M., Tóth, J., 2024. Rigorously proven chaos in chemical kinetics. Available as: <https://arxiv.org/abs/2402.18523>.
- [31] Dack, A., Qureshi, B., Ouldrige, T. E., Plesa, T. Recurrent neural chemical reaction networks that approximate arbitrary dynamics. Available as: <https://arxiv.org/abs/2406.03456>.
- [32] Sprott, J. C., 1994. Some simple chaotic flows. *Phys. Rev. E*, **50**, R647(R).
- [33] Narasimhan, R., 1985. Analysis on Real and Complex Manifolds, Second Edition. Elsevier Science.